Quaternary Science Reviews 346 (2024) 109082

Contents lists available at ScienceDirect

Quaternary Science Reviews

journal homepage: www.elsevier.com/locate/quascirev

Variation in the Quaternary *Stegodon-Ailuropoda* Faunal Complex in Southern China: Upper Pubu Cave (Bubing Basin, Guangxi)

Yijing Zhang [a], Yaobin Fan [a], Yanyan Yao [a,b], Chun Tian [a], Hua Liang [a], Jinyan Li [c], Wei Liao [a,**], Christopher J. Bae [d,***], Wei Wang [a,*]

[a] Institute of Cultural Heritage, Shandong University, 72 Jimo-Binhai Road, Qingdao, 266237, China
[b] Center for Paleoanthropology Research, Anthropology Museum of Guangxi, Nanning, China
[c] Tiandong County Museum, Tiandong, 531500, China
[d] Department of Anthropology, University of Hawai'i at Manoa, 2424 Maile Way 346 Saunders Hall, Honolulu, HI, 96822, USA

ARTICLE INFO

Handling editor: Rivka Rabinovich

Keywords:
"Stegodon-Ailuropoda" fauna
Late Middle Pleistocene
Evolutionary sequence
Upper Pubu Cave
Southern China

ABSTRACT

The *Stegodon-Ailuropoda* Faunal Complex is representative of Quaternary faunas across southern China. However, it is becoming increasingly clear that a great deal of variation is present within the faunal complex. Here we report a new late Quaternary faunal assemblage from Upper Pubu Cave, Bubing Basin, Guangxi, southern China. Upper Pubu is a good example of the variation in the *Stegodon-Ailuropoda* Faunal Complex, particularly when situated in the broader Bubing Basin Quaternary faunal sequence. Upper Pubu was excavated two times resulting in the discovery of 2396 mammalian fossils, consisting mostly of isolated teeth from medium- to large-sized animals. Twenty four mammalian taxa were identified, representative of the *Stegodon-Ailuropoda* Faunal Complex, including *Ailuropoda*, *Stegodon*, *Pongo*, *Rhinoceros*, *Tapirus*, and *Elephas*. Upper Pubu is dated to 210–100 ka by Uranium-series, electron spin resonance (ESR) and optically stimulated luminescence (OSL) methods. The Upper Pubu fossils largely date to Marine Isotope Stage ("MIS") 6. Given the severity of the climate during MIS 6, the reduction in both the number and proportion of primates and carnivores in Upper Pubu may be the result of environmental deterioration and a decrease in forested areas towards the end of the Middle Pleistocene ("Chibanian"). It is reasonable to speculate that a predominantly forested and mosaic-like habitat was present during the end of the Middle Pleistocene in southern China – a good example of environmental change during the Quaternary in the region.

1. Introduction

Since the beginning of the 20th century, paleontological investigations and discoveries led researchers to create the *Stegodon-Ailuropoda* Faunal Complex (SAFC) to be the representative (sub)tropical Pleistocene mammal assemblage in southern China (Colbert, 1942, 1943; Colbert and Hooijer, 1953; Kahlke, 1961). The representative faunas of SAFC encompass a range of sites, including Yenchingkou in Szechwan, Longgupo in Chongqing, Longgudong in Hubei, and Liucheng *Gigantopithecus* Cave, Liuzhou Bijiashan, Daxin Hei Cave (Black Cave) in Guangxi, as well as Hualongdong in Anhui (Colbert and Hooijer, 1953; Han, 1982, 1987; Han et al., 1975, 2017; Huang et al., 1995; Huang and Fang, 1991; Matthew and Granger, 1923; Pei and Woo, 1956; Tong et al., 2018; Tong and Guérin, 2009; Zheng, 2004). The chronological sequence of the SAFC has long been debated (Ji, 1977; Jin et al., 2008; Kahlke, 1961; Matthew and Granger, 1923; Pei, 1935; Zhou, 1957).

The geographic range of the SAFC however is quite interesting as it appears to not only be restricted to southern China. For instance, during the late Early Pleistocene, considerable numbers of typical southern taxa migrated northward through and around the Qinling Mountain Range (the geographical boundary between northern and southern China) into northern China, Korea, and Japan (Bae, 2024; Hu and Qi, 1978; Nakazawa and Bae, 2018; Norton, 2000; Norton et al., 2010; Qiu, 2006). Further, during the Middle Pleistocene the SAFC expanded southwards

* Corresponding author.
** Corresponding author.
*** Corresponding author.
E-mail addresses: yijingzhang@mail.sdu.edu.cn (Y. Zhang), fanyaobin11@mail.sdu.edu.cn (Y. Fan), yaoyanyan@amgx.org (Y. Yao), 202120267@mail.sdu.edu.cn (C. Tian), 1678521344@qq.com (H. Liang), liyan00c@163.com (J. Li), liaowei@sdu.edu.cn (W. Liao), cjbae@hawaii.edu (C.J. Bae), wangw@sdu.edu.cn (W. Wang).

https://doi.org/10.1016/j.quascirev.2024.109082
Received 25 April 2024; Received in revised form 28 June 2024; Accepted 9 November 2024
Available online 15 November 2024

into Mainland Southeast Asia (Suraprasit et al., 2016, 2021). However, the SAFC has traditionally been under-utilized in Quaternary studies, including paleoanthropology, given the paucity of radiometric dates. As such, researchers have observed that the simple broad use of the term SAFC tends to ignore spatial and temporal variability within the faunal complex (Wang et al., 2007).

Over the past two decades systematic field investigations and excavations were concentrated in the Chongzuo area and the Bubing Basin, Guangxi Zhuang Autonomous Region, southern China. The focus of this research was to investigate the vast limestone karst deposits in caves that may contain Quaternary faunas. The result has been the discovery of hundreds of cave sites in these two concentrated areas in Guangxi (Zhang et al., 2024). Among them, at least thirty two sites have reported secure and well-constrained ages (Table 1).

In the Chongzuo region, as the karst peaks have unvegetated sheer sides, the cave entrances are relatively easy to locate. A great number of Early Pleistocene faunas, that include *Gigantopithecus* fossils, were discovered in Chongzuo, and the biostratigraphic sequence and chronological framework were initially established accordingly (Jin et al., 2008, 2009b, 2014; Sun et al., 2014; Zhu et al., 2017). Middle Pleistocene fossil localities are the most abundant. The biostratigraphic age of the Yixiantian fauna was first considered to belong to the late Middle Pleistocene, which is consistent with the OSL dating results of 299 ± 50 ka (Pan, 2021; Pan et al., 2023). Nevertheless, the latest study reveals an earlier modeled upper age range of the Yixiantian faunal assemblage, suggesting that it may date back to the early Middle Pleistocene (Zhang et al., 2024). The Zhiren Cave was initially dated to 110 ka (Cai et al., 2017), however, more recent chronological research suggests the fossils were deposited between ~190 and ~130 ka, a much older age range (Ge et al., 2020). To date, Late Pleistocene sites published in this region are still limited, with only Yanlidong Cave (later stage), Xiaokou Cave and Yicun Cave having published results (Liao et al., 2022; Yao et al., 2020; Zhang et al., 2024).

In the Bubing Basin, a series of cave sites have been systematically investigated and excavated since 2000, leading to the discovery of a rich Quaternary mammal sequence (Table 1). In the karstic peaks of the Bubing Basin, there is a correlation between the elevation of the caves and the ages of the mammalian faunas they contain (Sun et al., 2014; Wang et al., 2007). In general, the higher caves are dated to the Early Pleistocene, while the caves located closer to current ground level are

Table 1
Background information of the cave sites reported in the Chongzuo region and the Bubing Basin.

Region	Geological Age	Fossil Site	Estimated Age	Dating Method	Reference
Chongzuo	Early Pleistocene	Baikong Cave	2.58–1.95 Ma; ~2.0 Ma	Magneto-biostratigraphy	Harrison et al. (2014), 2021; Jin et al. (2014); Sun et al. (2014)
		Yanliang Cave	~2.0 Ma; 0.87–0.21 Ma	Biostratigraphy; U-series; coupled ESR/U-series; pIR-IRSL	Yan et al. (2014); Zhang et al. (2024); Zhu et al. (2017)
		Juyuan Cave	1.95–1.78 Ma; ~1.8 Ma	Magneto-biostratigraphy	Harrison et al. (2014), 2021; Sun et al. (2014); Wang et al. (2017a)
		Sanhe Cave	1.78–1.07 Ma; ~1.2 Ma; 0.91–0.6 Ma	coupled ESR/U-series; Magneto-biostratigraphy	Harrison et al. (2021); Shao et al. (2015); Jin et al. (2014); Sun et al. (2014); Wang et al. (2014)
		Queque Cave	1.48–0.55 Ma; 1.07–0.99 Ma; ~1.0 Ma	Magneto-biostratigraphy	Dong et al. (2020); Jin et al. (2014); Sun et al. (2014); Zhang et al. (2024)
		Zhanwang Cave	1.3–0.24 Ma	U-series; pIR-IRSL; coupled ESR/U-series	Zhang et al. (2024)
	Middle Pleistocene	Yanlidong Cave (early stage)	~600 ka	U-series	Yao et al. (2023)
		Bapeng Cave	406-298 ka	U-series; pIR-IRSL; coupled ESR/U-series	Zhang et al. (2024)
		Hejiang Cave	400-320 ka; 321-250 ka	U-series; pIR-IRSL; coupled ESR/U-series	Zhang et al. (2014), 2024
		Daxin Hei Cave (Black Cave)	883-357 ka; 404-382 ka; 380-308 ka	U-series; coupled ESR/U-series	Rink et al. (2008); Shao et al. (2017); Zhang et al. (2024)
		Yixiantian Cave	889-255 ka; ~300 ka	U-series; pIR-IRSL; OSL	Pan (2021); Pan et al. (2023); Zhang et al. (2024)
		Shuangtan Cave	342-242 ka	U-series; pIR-IRSL; coupled ESR/U-series	Zhang et al. (2024)
		Gongjishan Cave	292-159 ka	pIR-IRSL	Zhang et al. (2024)
		Quzai Cave	235-166 ka	pIR-IRSL	Zhang et al. (2024)
		Baxian Cave	232-129 ka	U-series; pIR-IRSL; OSL coupled ESR/U-series	Zhang et al. (2024)
		Mafeng Cave	193-138 ka	U-series; pIR-IRSL; OSL	Zhang et al. (2024)
		Zhiren Cave	190-130 ka; 116-106 ka; 111 ka	U-series; OSL	Cai et al. (2017); Ge et al. (2020); Jin et al. (2009a); Liu et al. (2010)
	Late Pleistocene	Yanlidong Cave (later stage)	<186 ka; 65-30 ka	U-series; OSL	Yao et al. (2020)
		Xiaokou Cave	96-79 ka	U-series; pIR-IRSL; OSL	Zhang et al. (2024)
		Yicun Cave	66-57 ka	U-series	Liao et al. (2022)
Bubing Basin	Early Pleistocene	Chuifeng Cave	1.92–1.38 Ma; 2.31–1.04 Ma	ESR; U-series; magnetostratigraphy	Shao et al. (2014); Zhang et al. (2024)
		Mohui Cave	1.95–1.78 Ma; 1.91–1.18 Ma	coupled ESR/U-series; Magneto-biostratigraphy	Shao et al. (2015); Sun et al. (2017)
	Middle Pleistocene	Upper Wuyun Cave	~0.7 Ma	Magneto-biostratigraphy	Sun et al. (2017)
		Shizi Cave	517-366 ka	U-series	Kong et al. (2012)
		Ganxian Cave	362-169 ka	U-series; coupled ESR/U-series	Liang et al. (2022), 2023
		Wuyun Cave	300-250 ka; 211-60 ka	U-series	Wang et al. (2007); Zhang et al. (2024)
		Zhongshan Cave	246-64 ka	U-series; pIR-IRSL	Zhang et al. (2024)
	Late Pleistocene	Luna Cave	127-70 ka; ~97 ka; >78 ka	U-series; OSL	Bae et al. (2014); Sun et al. (2021a,b)
		Lower Pubu Cave	77-21 ka	OSL	Zhang et al. (2024)
		Baolai Cave	54-24 ka	U-series	Fan et al. (2022a)
		Lumei	49-24 ka	pIR-IRSL	Zhang et al. (2024)
	Holocene	Cunkong Cave	Late Holocene	Biostratigraphy	Wang et al. (2007)

placed in the Late Pleistocene. This may be related to a late uplift of the mountains in the basin, but more likely, extensive river downcutting during the Quaternary. As a result, based on faunal correlations and multi-method dating, a basic time scale for the biostratigraphy of Pleistocene mammalian faunas in the Bubing Basin has been established (Deng et al., 2019; Rink et al., 2008; Sun et al., 2017; Wang et al., 2007).

The faunal assemblages from Chongzuo and Bubing provide important paleontological evidence for our understanding of Quaternary mammalian evolution in the region. However, discontinuities in cave deposition have resulted in some temporal gaps in the faunal record of this region; particularly, the Early-Middle Pleistocene transition, the Middle-Late Pleistocene transition, and the Pleistocene-Holocene transition. In order to partially rectify this problem, here we report a newly discovered terminal Middle Pleistocene mammalian fauna from the Upper Pubu Cave in the Bubing Basin, western Guangxi. To date, no taxonomic analysis of the Upper Pubu fossils has been conducted, but the dating results have been published. The initial ESR study estimated the age of the Upper Pubu faunal assemblage to be between 88 and 280 ka (Rink et al., 2008). However, a recent study using luminescence dating techniques (both pIR-IRSL dating of feldspars and optically stimulated luminescence of quartz) on the sediments as well as U-series dating on flowstones has refined this age range to 210–100 ka (Zhang et al., 2024). Here, we describe the geological context of the Upper Pubu site and present a detailed taxonomic analysis of the fossils. Finally, in comparison with some well-documented Middle and Late Pleistocene faunas from southern China and Southeast Asia, the contribution of the Upper Pubu fauna for understanding broader environmental changes during the Middle and Late Pleistocene is discussed. The Upper Pubu fossils help fill the Pleistocene mammal gap in the Middle-Late Pleistocene transition in the region and also provide new insights into variation in the *Stegodon-Ailuropoda* Faunal Complex in southern China.

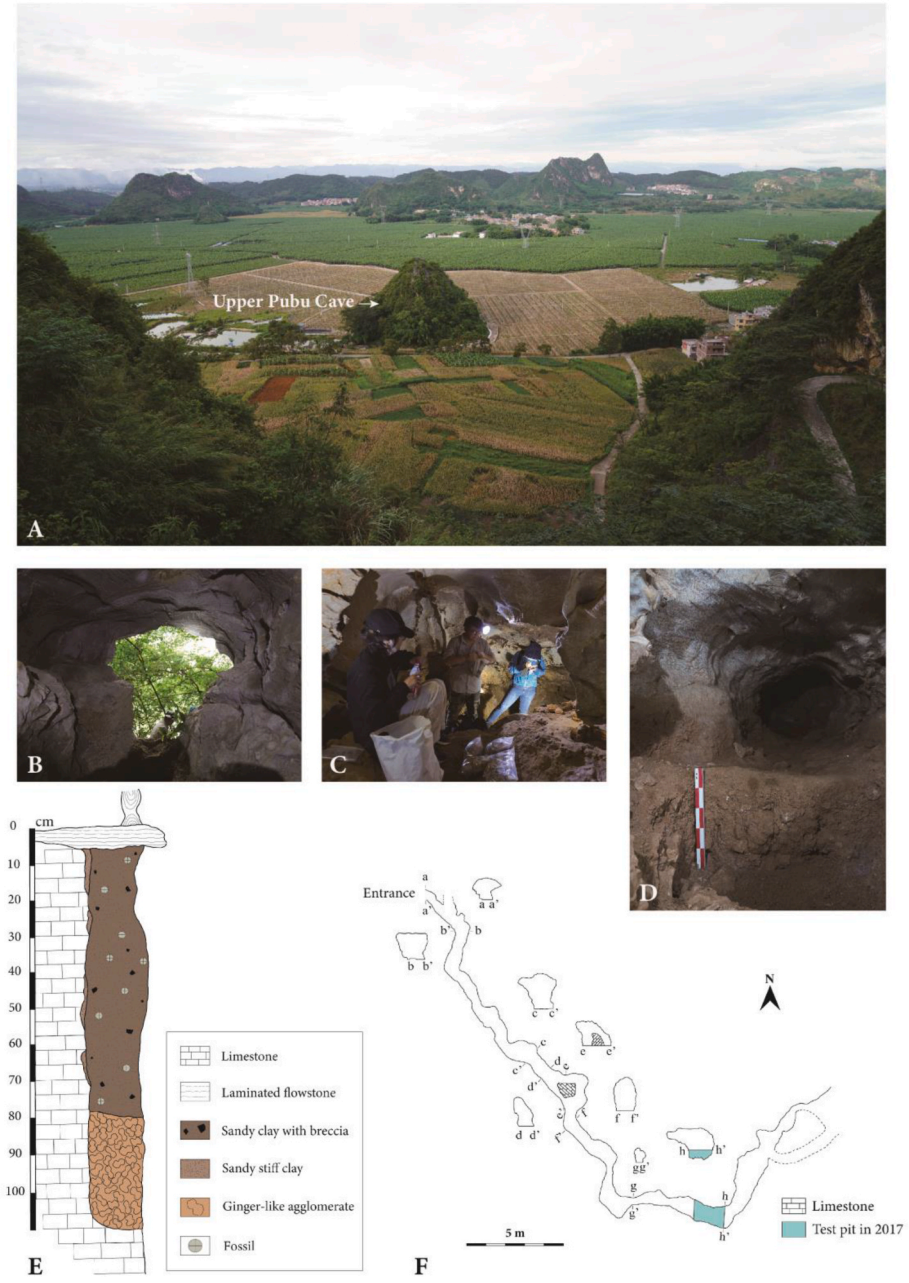

Fig. 1. Upper Pubu Cave. A, Landscape of the surrounding area and location of Upper Pubu (from south to north); B, Cave entrance (viewed from the inside); C, Sampling and recording; D, The west profile of the test pit in 2017; E, The stratigraphic section (based on the south wall of the test pit in 2017); F, Plan of Upper Pubu.

2. Geological background

2.1. Location and geological setting

Upper Pubu Cave (23°53.300′N, 106°59.167′E) is located in the southeast part of the Bubing Basin about 500 m from Pubu Village (Fig. 1A). The cave developed in an isolated karst peak of Permian limestone, and the limestone hill is around 100 m east-west and 80 m north-south. The cave entrance is on the west side of the hill, 15 m above the local river level (Fig. 1B). The corridor of the Upper Pubu Cave is long and quite narrow, about 0.5–1.5 m in width, ~1–3 m in height and ~36 m in depth. At the end of the corridor, there is a nearly vertically developed large cavern that is about 10 m deep. The cavern connects the Upper and Lower Pubu caves, forming a cave system that includes two horizontally developed caves. The entrance to the Lower Pubu Cave is ~10 m directly below Upper Pubu. Lower Pubu was reported previously by Wang et al. (2007).

Upper Pubu was discovered by a survey team from the Natural History Museum of Guangxi in 2002. Subsequently, more than 1800 mammalian fossils were collected from the slightly disturbed sediment at the terminal end of the corridor. To verify the origin of the fossils, a formal excavation was conducted in November 2017 by the Anthropology Museum of Guangxi (Fig. 1C-D, F). The 2017 excavation resulted in the discovery of about 540 isolated fossil teeth *in situ*. The fossils obtained from these two separate field seasons do not differ in faunal composition. Further, the fossils in the test pit originated from the same stratum as the earlier fieldwork. Thus, we treat the two separate fossil assemblages as one homogeneous faunal accumulation.

2.2. Stratigraphy

The Upper Pubu sediments are well-preserved and virtually undisturbed in all areas of the corridor. Three stratigraphic layers are identified from top to bottom (Fig. 1E):

Layer 1: White laminated flowstone, each sub-layer is about 0.5 cm in thickness, and more than 6 sub-layers were identified. 2–5 cm in total thickness;

Layer 2: Light brown silty clay with breccia, which contains fossiliferous calcareous cementation and yielded abundant mammalian fossil teeth. 67–87 cm in total thickness;

Layer 3: Light brown sandy clay with yellow ginger-like conglomerates without any fossils. ~30 cm in total thickness.

In addition, a little yellowish-brown and calcareous cemented sandy clay is adhered to the walls of the cave in an angular unconformity. Although not widespread, it is undoubtedly a remnant of an earlier filling of the cave.

The age of the Upper Pubu faunal assemblage was initially estimated to be between 88 and 280 ka based on ESR dating (Rink et al., 2008). Recently, OSL dating of the sediments and U-series dating of the flowstone produced a narrower age range of 210–100 ka (Zhang et al., 2024).

3. Material and methods

3.1. Material

To date, a total of 2396 isolated teeth of medium and large mammals were identified from Upper Pubu. Unfortunately, no osseus fossils were found except a few petrosal bones. All fossil specimens are curated in the Natural History Museum of Guangxi (Nanning) and the Laboratory of Human Evolution at Shandong University (Qingdao).

3.2. Methods

Specimens were coded differently depending on which team collected and curated the fossils. For instance, "UPB" (Upper Pubu) with catalog numbers starting from UPB001 to UPB541 are present, as well as "TPB" (Top Pubu) from TPB001 to TPB069, and simply a string of numbers that starts with "02" from 024751 to 025124, and from 025164 to 026579 are present.

Each fossil tooth, considered as one specimen, was identified at the species or genus level (at least to family level). These identifications are based on morphologic characters and metric dimensions and compared with samples from other related faunas. Dental morphologic characters follow Swindler (2002) for primates, Maglio (1973), Roth and Shoshani (1988), Van den Bergh (1999), and Wang et al. (2017a,b) for proboscideans, Jiangzuo et al. (2019) for ursids, Jiangzuo et al. (2018a,b) for mustelids, Tong (2005) for tapirids, Yan et al. (2014) for rhinocerotids, van der Made (1996) and Sun et al. (2021a,b) for suids, Zhang et al. (2018a,b) for cervids, and Suraprasit et al. (2016) for ruminants.

After identification, the Upper Pubu assemblage was compared with those from Ganxian and Baxian in detail and, when applicable, with some other Middle and Late Pleistocene mammalian faunas of known age in both southern China and southeast Asia, including: Middle Pleistocene sites of Yixiantian Cave, Wuyun Cave and Diaozhongyan Cave, and Late Pleistocene sites of Fuyan Cave, Mocun Cave, Baolai Cave in southern China; Middle Pleistocene sites of Coc Muoi Cave in northern Vietnam, Ngalau Gupin Cave in Sumatra; Late Pleistocene sites of Duoi U'Oi and Ma U'Oi Caves in northern Vietnam, Nam Lot Cave in northern Laos, and Punung in Java. The number of identifiable specimens (NISP) and minimum number of individuals (MNI) were tabulated to show their proportions. The taxonomic breakdown and NISP/MNI counts are presented in Tables 2–4.

Tooth dimensions (lengths and widths) of the Upper Pubu fossil teeth were measured using digital calipers to the nearest 0.01 mm. The maximum length (L) was taken along the mesial-distal margins, while the maximum width (W) from the labial (for incisors and canines)/buccal (for premolars and molars) to lingual margins. In the case of the Perissodactyla cheek teeth, anterior width (AW) and posterior width (PW) were recorded respectively. Uppercase letters were used for upper teeth (I/C/P/M) while lowercase letters for lower ones (i/c/p/m). The prefix "D/d" refers to upper/lower deciduous teeth. For example, a third deciduous lower right premolar is recorded as Rdp3. The raw metric

Table 2
The number of identifiable specimens (NISP) and the minimum number of individuals (MNI) of different taxa and their proportion (NISP% & MNI%) in the Upper Pubu fauna.

Taxa in the Upper Pubu Cave	NISP	NISP%	MNI	MNI%
Pongo sp.	11	0.46%	3	1.26%
Nomascus sp.	1	0.04%	1	0.42%
Macaca sp.	11	0.46%	2	0.84%
Trachypithecus sp.	1	0.04%	1	0.42%
Cercopithecidae gen. et sp. indet.	2	0.08%	1	0.42%
Hystrix subcristata	54	2.25%	7	2.93%
Atherurus sp.	5	0.21%	3	1.26%
Stegodon sp.	13	0.54%	1	0.42%
Elephas maximus	2	0.08%	2	0.84%
Arctonyx collaris	7	0.29%	3	1.26%
Neofelis nebulosa	2	0.08%	1	0.42%
Ailuropoda melanoleuca baconi	14	0.58%	3	1.26%
Ursus thibetanus	36	1.50%	9	3.77%
Ursus (Helarctos) malayanus	6	0.25%	4	1.67%
Carnivora indet.	2	0.08%	2	0.84%
Tapirus sinensis	9	0.38%	4	1.67%
Rhinoceros sondaicus	10	0.42%	3	1.26%
Rhinoceros sp.	12	0.50%	4	1.67%
Dicerorhinus sumatrensis	7	0.29%	2	0.84%
Cervus (Rusa) unicolour	911	38.02%	76	31.80%
Cervidae gen. et sp. indet.	7	0.29%	/	/
Elaphodus cephalophus	104	4.34%	11	4.60%
Muntiacus muntjak	230	9.60%	23	9.62%
Muntiacus reevesi	5	0.21%	2	0.84%
Bos gaurus	43	1.79%	8	3.35%
Capricornis sumatraensis	23	0.96%	6	2.51%
Sus scrofa	868	36.23%	57	23.85%
Total	**2396**	100.00%	**239**	100.00%

Table 3
Composition of the Upper Pubu faunal assemblage (Primates, Rodentia, Proboscidea, Carnivora, Perissodactyla, and Artiodactyla) with that of some Middle Pleistocene to Late Pleistocene sites in South China: Yixiantian Cave (Pan et al., 2023), Ganxian Cave (Liang et al., 2022), Wuyun Cave (Chen et al., 2002), Baxian Cave (Zhang et al., 2024), Diaozhongyan Cave (Liang et al., 2020), Fuyan Cave (Li et al., 2013), Mocun Cave (Fan et al., 2022b), Baolai Cave (Fan et al., 2022a), and Cunkong Cave (Wang et al., 2007). Names in bold indicate global extinction; The asterisk (*) indicates local extinction.

		Yixiantian Cave	Ganxian Cave	Wuyun Cave	Baxian Cave	Diaozhongyan Cave	Upper Pubu Cave	Fuyan Cave	Mocun Cave	Baolai Cave	Cunkong Cave
		889-255 ka	360 ka - 160 ka	350-200 ka	232-129 ka	231-205 ka	210–100 ka	120-80 ka	101-66 ka	54-24 ka	Holocene
Primates	*Gigantopithecus blacki*	✓									
	**Pongo pygmaeus/ P. weidenreichi*	✓	✓	✓							
	**Pongo* sp.				✓		✓		✓		
	Homo				✓						✓
	Nomascus/ Hylobates sp.	✓	✓		✓	✓	✓	✓	✓		
	Macaca sp.	✓	✓	✓	✓	✓	✓	✓	✓	✓	✓
	Pygathrix sp.	✓			✓					✓	
	Rhinopithecus sp.	✓			✓						
	Trachypithecus sp./ *Presbytis* sp.	✓	✓	✓	✓	✓	✓	✓	✓		
Rodentia	***Hystrix magna***								✓		
	Hystrix subcristata/ sp.	✓	✓	✓	✓	✓	✓	✓	✓	✓	✓
	Atherurus macrourus/sp.	✓		✓	✓		✓			✓	
Proboscidea	***Stegodon orientalis*/sp.**	✓	✓	✓	✓	✓	✓	✓	✓	✓	
	**Elephas maximus/* sp.	✓	✓	✓	✓		✓	✓	✓		✓
Carnivora	**Cuon alpinus/C. alpinus antiquus*	✓	✓	✓							
	Cuon javanicus							✓			
	Cuon sp.				✓				✓	✓	
	Paguma larvata	✓			✓						
	Mustela sp.				✓						
	Martes flavigula/sp.				✓			✓			
	Melogale moschata/ sp.	✓			✓						
	Lutra lutra/sp.	✓			✓			✓			
	Herpestes sp.	✓			✓						
	Arctonyx collaris (rostratus)	✓	✓	✓	✓	✓	✓	✓	✓	✓	
	Melogale moschata	✓			✓						
	Viverra sp.	✓			✓			✓	✓		
	Viverricula sp.							✓			
	Chrotogale sp.				✓						
	Felis teilhardi			✓							
	**Felis(Panthera) tigris*	✓	✓	✓				✓		✓	✓
	Catopuma temminckii	✓			✓						
	Panthera cf. *pardus*	✓									
	Paradoxurus cf. *hermaphroditus*			✓					✓		
	Neofelis nebulosa	✓	✓		✓		✓		✓	✓	
	Prionailurus sp.				✓						
	Felis cf. *chaus*	✓			✓						
	Panthera pardus/sp.			✓	✓			✓		✓	
	Prionailurus bengalensis							✓			
	Crocuta ultima		✓					✓	✓		
	Crocuta crocuta				✓						
	Ailuropoda melanoleuca baconi	✓	✓	✓		✓	✓	✓			
	**Ailuropoda* sp.				✓				✓	✓	
	Ursus thibetanus	✓	✓	✓	✓	✓	✓	✓	✓	✓	✓
	**Ursus (Helarctos) malayanus*	✓			✓		✓				
Perissodactyla	***Megatapirus augustus***	✓	✓	✓	✓			✓	✓		
	Tapirus sinensis		✓	✓		✓	✓		✓		
	Rhinoceros sinensis			✓		✓					

(*continued on next page*)

Table 3 (*continued*)

		Yixiantian Cave	Ganxian Cave	Wuyun Cave	Baxian Cave	Diaozhongyan Cave	Upper Pubu Cave	Fuyan Cave	Mocun Cave	Baolai Cave	Cunkong Cave
		889-255 ka	360 ka - 160 ka	350-200 ka	232-129 ka	231-205 ka	210–100 ka	120-80 ka	101-66 ka	54-24 ka	Holocene
	**Rhinoceros sondaicus*	✓	✓				✓				
	**Rhinoceros* sp.		✓		✓		✓		✓	✓	
	**Dicerorhinus sumatrensis*		✓				✓	✓			
Artiodactyla	*Cervus (Rusa) unicolour*/sp.	✓	✓	✓	✓	✓	✓	✓	✓	✓	✓
	Cervus nippon							✓			
	Elaphodus cephalophus	✓			✓		✓			✓	
	Muntiacus muntjak/sp.	✓	✓	✓	✓	✓	✓	✓	✓		✓
	Muntiacus reevesi	✓	✓		✓		✓		✓	✓	
	Moschus sp.				✓			✓			
	Megalovis guangxiensis	✓	✓								
	Bubalus arnee		✓								
	Bos (Bibos) gaurus	✓	✓				✓	✓			
	Bos (Bibos) sp.				✓				✓		
	Bovinae gen. et sp. indet.			✓		✓				✓	✓
	**Capricornis sumatraensis*/sp.	✓	✓	✓	✓		✓	✓		✓	
	Caprinae gen. et sp. indet.					✓			✓		
	Sus xiaozhu	✓	✓						✓	✓	
	Sus peii	✓									
	Sus* cf. *australis							✓			
	Sus scrofa		✓	✓	✓	✓	✓	✓	✓	✓	✓

Table 4
The number of identifiable specimens (NISP) and the minimum number of individuals (MNI) of different orders and families and their percentage (NISP% & MNI%) of the Upper Pubu Cave, Ganxian Cave and Baxian Cave (Liang et al., 2022; Zhang et al., 2024).

Order	Family	NISP/NISP%	MNI/MNI%	NISP/NISP%	MNI/MNI%	NISP/NISP%
		Upper Pubu Cave		Ganxian Cave		Baxian Cave
Artiodactyla	**Total of Artiodactyla**	2191/91.4	183/76.6	1562/66.3	158/58.7	6893/58.4
	Suidae	868/36.2	57/23.9	533/22.6	40/14.9	3396/28.8
	Cervidae	1257/52.5	112/46.9	942/40.0	99/36.8	2269/19.2
	Bovidae	66/2.8	14/5.9	87/3.7	19/7.1	1227/10.4
	Moschidae	0	0	0	0	1
Perissodactyla	**Total of Perissodactyla**	38/1.6	13/5.4	64/2.7	16/5.9	121/1.0
	Rhinocerotidae	29/1.2	9/3.8	57/2.4	14/5.2	101/0.9
	Tapiridae	9/0.4	4/1.7	7/0.3	2/0.7	20/0.2
Proboscidea	**Total of Proboscidea**	15/0.6	3/1.3	23/1.0	3/1.1	224/1.9
	Stegodontidae	13/0.5	1/0.4	13/0.6	1/0.4	45/0.4
	Elephantidae	2/0.1	2/0.8	10/0.4	2/0.7	179/1.5
Carnivora	**Total of Carnivora**	67/2.8	22/9.2	127/5.4	29/10.8	932/7.9
	Canidae	0	0	2/0.1	1/0.4	10/0.1
	Ursidae	56/2.3	16/6.7	84/3.6	12/4.5	496/4.2
	Mustelidae	7/0.3	3/1.3	24/1.0	11/4.1	313/2.7
	Herpestidae	0	0	0	0	19/0.2
	Hyaenidae	0	0	4/0.2	1/0.4	1
	Felidae	2/0.1	1/0.4	13/0.6	4/1.5	74/0.6
	Viverridae	0	0	0	0	19/0.2
Rodentia	**Total of Rodentia**	59/2.5	10/4.2	363/15.4	37/13.8	1917/16.3
	Hystricidae	59/2.5	10/4.2	363/15.4	37/13.8	1917/16.3
Primates	**Total of Primates**	26/1.1	8/3.3	218/9.2	26/9.7	1709/14.5
	Hominidae	11/0.5	3/1.3	106/4.5	11/4.1	355/3.0
	Hylobatidae	1	1/0.4	4/0.2	1/0.4	13/0.1
	Cercopithecidae	14/0.6	4/1.7	108/4.6	14/5.2	1341/11.4
Total of all taxa		**2396**	**239**	**2357**	**269**	**11796**

data for all of the taxa and comparative fossil samples are presented in the Supplementary Online Material (Tables S1–S20).

4. Results

4.1. Taxonomic identifications

A total number of 2396 isolated teeth of medium and large mammals

have been identified to the family, genus or species level.

4.1.1. Primates

Pongo sp.: Eleven isolated teeth were collected, including one deciduous premolar (one dp4), two incisors (one I1 and one i2), one canine sexed to female, three premolars (one P4 and two p3s) and 4 M (two M2s, one M3 and one m2). The dp4 has a rectangular occlusal outline with five cusps (metaconid, entoconid, protoconid, hypoconid and hypoconulid) (Fig. 2A). The protoconid and metaconid are connected by a double transverse crest. A mesial fovea is present while a distal fovea is absent. The I1 has a typical shovel shape, with the mesiodistal diameter widening from the base of the crown to the top, and the widest buccolingual diameter is at the base of the crown. As the I1 is heavily worn, the development of a cingulum cannot be observed (Fig. 2B). The P4 displays two main cusps, and the crown has an oval shape (Fig. 2C). The paracone is separated from the protocone by a distinct curved groove developed mesiodistally. The crown of M2s is a rounded rectangular shape that is mainly composed of four cusps (Fig. 2D). The M2 can be distinguished from the M1 by a larger protocone and a reduced hypocone (Liang et al., 2023). Further, there is a tapering effect toward the distal end of the M2, which is different from the nearly parallel two sides of the M1 (Hooijer, 1948). In the M2s, the crista obliqua (postprotocrista) join the protocone and metacone, and the transverse crest is visible in one specimen, while the other is not observable as it is heavily worn and fragmentary. The M3 is identified by a notable reduction in the size of the metacone and the hypocone when compared to the M2s. In

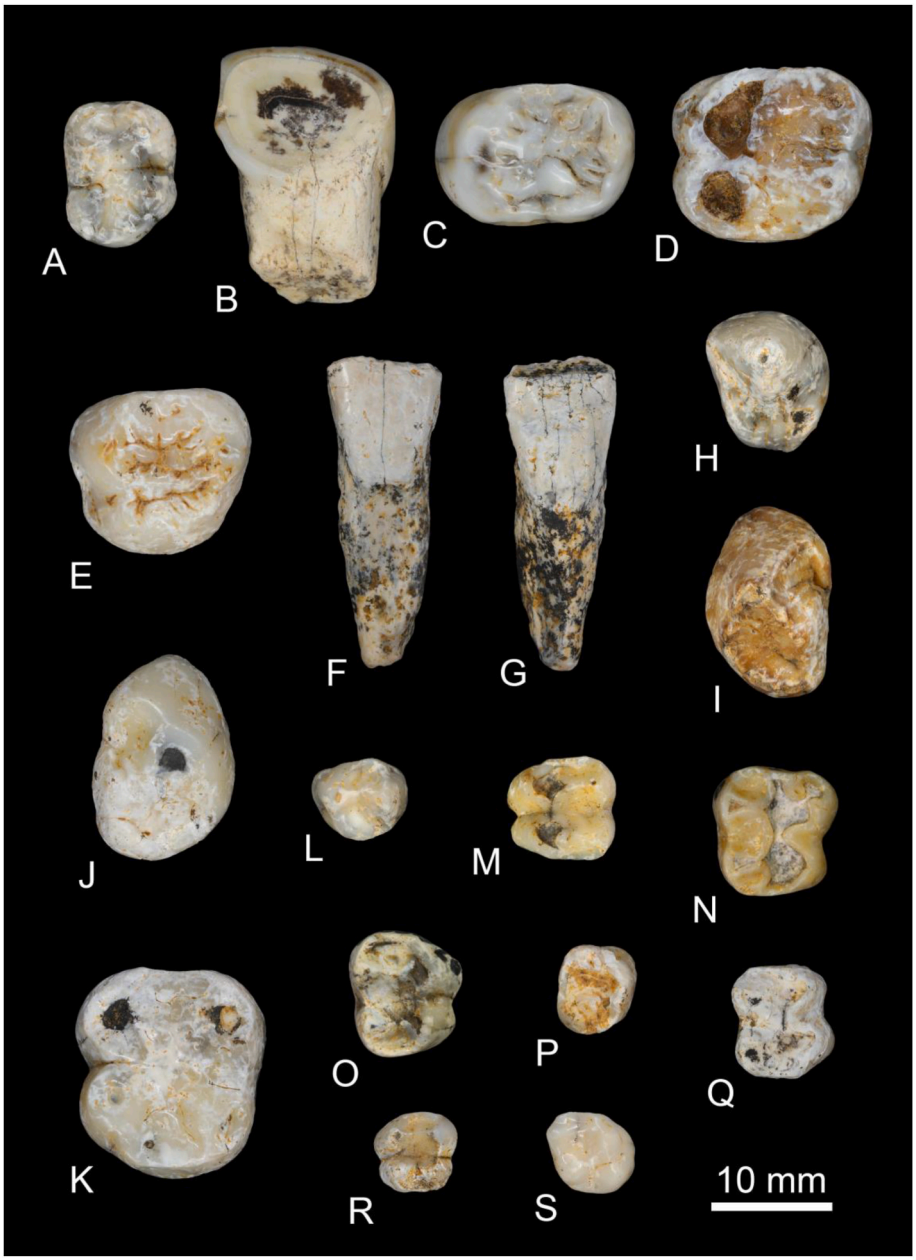

Fig. 2. Primates from Upper Pubu Cave. *Pongo* sp.(A-K): A, Right dp4 (UPB143) in occlusal view; B, Left I1 (TPB026) in lingual view; C, Left P4 (TPB023) in occlusal view; D, Left M2 (TPB024) in occlusal view; E, Left M3 (UPB299) in occlusal view; F-G, Left i2 (TPB025) in labial (F) and lingual (G) views; H, Right c (UPB519) of female in occlusal view; I, Left p3 (UPB517) in occlusal view; J, Right p3 (UPB140) in occlusal view; K, Left m2 (UPB300) in occlusal view. *Macaca* sp. (L-Q): L, Left P4 (UPB148) in occlusal view; M, Left M1 (025082) in occlusal view; N, Right M2 (025079) in occlusal view; O, Right M3 (025081) in occlusal view; P, Right p4 (UPB514) in occlusal view; Q, Right m2 (UPB510) in occlusal view. *Trachypithecus* sp. (R): R, Left M1 (UPB305) in occlusal view. *Nomascus* sp. (S): S, Right M2 (UPB142) in occlusal view.

the specimen UPB299, a well-defined mesial fovea is expressed. The crista obliqua cannot be found while two transverse crests are present in UPB299 (Fig. 2E). These character traits are actually exceptions for the morphology of the M3 more generally, differing from those of the M3s from Ganxian Cave (Liang et al., 2023), Yicun Cave (Liao et al., 2022), Baikong Cave (Harrison et al., 2021), Queque Cave (Harrison et al., 2014) and Sanhe Cave (Wang et al., 2014). The lingual cingulum is not present in the M3.

The crown of the *Pongo* i2 is relatively narrow and high, and the mesio-distal diameter widens from the base of the crown toward the incisal edge, with the widest buccolingual diameter located at the base of the crown (Fig. 2F–G). Based on *Pongo* sexual dimorphism more generally (Hooijer, 1948) and the dimensions of this specific specimen, the i2 is assumed to have belonged to a female individual (Fig. 2H). The mesio-lateral surface of the canine is relatively flat. A well-developed cingulum ascends gradually from the postero-lingual angle to the antero-lingual angle forming a well-marked oblique ledge. The p3s develop a high main cusp located at the central buccal side forming a pyramidal crown with a subtriangular outline in occlusal view (Fig. 2I–J). Their structures are also characterized by three ridges extending from the apex of the protoconid. A lingual cingulum is present near the base of the crown. The occlusal outline of the m2 is sub-rectangular, and the external contour is concave between the metaconid and entoconid (Fig. 2K). The m2 has five main cusps showing a Y-5 groove pattern. The metaconid is the highest and most developed cusp while the hypoconulid is the smallest. A small and shallow fossa is present in the anterior part of the crown. The general morphological characteristics of the Upper Pubu specimens is similar to the basic characteristics of *Pongo*. Although the dental size ranges of the specimens have a considerable overlap with those from Ganxian (Liang et al., 2023) and Yixiantian (Pan et al., 2023) (Table S1), considering that the number of Upper Pubu specimens is very limited (only ten, plus one fragmentary one), these fossils are temporarily assigned to *Pongo* sp.

Macaca sp.: Eleven isolated permanent teeth, one upper premolar, six upper molars, two lower premolars and two lower molars, are attributed to the genus *Macaca*. The crown of the P4 is of medium height, with an oval occlusal surface and a slightly flattened external profile on the distal side (Fig. 2L). It has two cusps: the paracone on the buccal side is higher than the protocone on the lingual side. A transverse crista between the two cusps divides the occlusal surface into a smaller mesial fovea and a larger distal fovea. All of the upper molars (three M1s, two M2s and one M3) display a bilophodont structure (Fig. 2M-N). The M2s have a more developed mesial shelf compared to the M1s. An interconulus exists on the lingual surface of the only M3 (Fig. 2O). The p4s are heavily worn (Fig. 2P). Only one specimen preserves the trace of the protocristid. The crown of the m2s is sub-rectangular in outline, with four cusps connected by two transverse cristae and a deep fossa between them (Fig. 2Q). Both the mesial shelf and the distal shelf are well-developed. The angle between the metaconid and the entoconid in the lingual view is a large acute angle. The metric dimensions of the teeth are presented in Table S2 and there is a large overlap with those from Longgudong (Zheng, 2004), Mohui (Wang, 2013), Yanlidong (Yao et al., 2023), Ganxian (Liang et al., 2022) and Mocun Caves (Fan et al., 2022b). Therefore, we preferentially assign these Upper Pubu specimens to *Macaca* sp.

Trachypithecus sp.: One upper colobine molar exhibiting a bilophodont pattern was identified. The cusps are sharper than those of the genus *Macaca*, the latter's cusps normally developing on a rounded subtrapezoidal occlusal surface (Fig. 2R). The mesial shelf is narrow and long and the ridges are sharp. The lingual groove is deep. A contraction appears at the cervical line. For comparison, the Chongzuo colobine fossils were assigned to three distinct groups according to their size: *Rhinopithecus*, which consisted of larger-sized specimens; *Pygathrix*, which included medium-sized specimens; and *Trachypithecus*, which comprised smaller-sized specimens (Takai et al., 2014). The dimensions of the Upper Pubu fossil fall within the range of fossil *Trachypithecus* from Yixiantian Cave (Pan et al., 2023) and extant individuals, and are also similar to *Trachypithecus francoisi* from Luoding (Gu et al., 1996). Based on the morphology and dimensions of the single collected tooth (Table S3), we temporarily identify it as *Trachypithecus* sp.

Nomascus sp.: One isolated permanent M2 is attributed to the genus *Nomascus*. The M2 shows a rhombic occlusal outline, with a well-developed mesial shelf and four cusps (Fig. 2S). The mesial margin is basically parallel to the distal one. The paracone is the highest, separated from the protocone by the anterior central sulcus. A crista obliqua extends from the protocone to connect the metacone. Traces of the cingulum are visible on the lingual side of the protocone. The mesio-distal length of the Upper Pubu M2 falls within the range of the *Nomascus* fossils from Yixiantian Cave, but its width is slightly shorter (Pan et al., 2023). Further, the dimensions of the Upper Pubu M2 are moderately smaller than the fossil specimens from Jiulengshan Hill (Zhao et al., 1981), fossils from some cave sites in the Chongzuo area (Zhang et al., 2018b), and those described by Gu in the 1980s (Gu, 1986). Due to the limited sample size, the tooth is cautiously assigned to *Nomascus* sp. (Table S4).

Cercopithecidae gen. et sp. indet.: Two lower molars are assigned to Cercopithecidae gen. et sp. indet. However, precise taxonomic identification is challenging due to their heavily worn and fragmented condition.

4.1.2. Rodentia

Hystrix subcristata: 54 isolated teeth are assigned to *Hystrix subcristata* based primarily on their size (Table S5). Compared with mandibular incisors, maxillary incisors are more robust and curved (Fig. 3B–C). Their cross sections are all nearly rounded triangles. The enamel of the incisors only covers the labial side and the medial and lateral front of the teeth. The maxillary premolars and molars are significantly curved on the buccal side, with a deep hypoflexus opening backward on the lingual side, and three shallow folds (paraflexus, mesoflexus and metaflexus) developed on the buccal side (Fig. 3E). On the contrary, the hypoflexid is present on the buccal side of the mandibular teeth (Fig. 3F–H), with three shallow lingual folds (paraflexid, mesoflexid and metaflexid). Enamel rings can be seen on the occlusal surface given the heavy wear that is present. The dimensions of the Upper Pubu *H. subcristata* teeth are slightly larger than those from Longgupo (Huang and Fang, 1991) and overlap with those from Ganxian (Liang et al., 2022) and Mocun (Fan et al., 2022b).

Atherurus sp.: Five porcupine incisors, much smaller in size and with thinner enamel than those attributed to *Hystrix subcristata*, were recovered in Upper Pubu (Fig. 3A–D). These characters are relatively similar to those of *Atherurus*. Although no cheek teeth of the same taxon were

Fig. 3. Rodentia from Upper Pubu Cave. *Atherurus* sp. (A, D): Left i (UPB470) in mesial (A) and distal (D) views. *Hystrix subcristata* (B-C, E-H): B-C, Right I (UPB438) in distal (B) and mesial (C) views; E, Left M1/2 (UPB484) in occlusal view; F, Right p4 (UPB454) in occlusal view; G, Right m1/2 (UPB460) in occlusal view; H, Left m3 (UPB458) in occlusal view.

found in Upper Pubu, these incisors are assigned to *Atherurus* sp.

4.1.3. Proboscidae

Stegodon sp.: Thirteen fossils with low crowns are attributed to *Stegodon* (two incomplete teeth, two isolated lamellae, and nine tooth fragments). Only one specimen (UPB493) preserves the last ridge-shaped loph and the posterior talon can be recognized as an upper first molar (Fig. 4D–F). Other specimens are unidentifiable, but can still be estimated to be parts of permanent teeth on account of the thickness of their enamel layers. The last loph consists of more than nine slightly worn mammillae, while the posterior talon contains four mammillae and one isolated mammilla is present on the buccal side. Both of them developed several smaller mammillae. The maximum width of UPB493 is 68.45 mm. The bases between the lophs are connected, and the valleys between the lophs are V-shaped in lateral view and partially filled with cement. The characteristics and measurements of the Upper Pubu specimens are consistent with the *Stegodon* fossils described from Mawokou Cave in Bijie (Wang et al., 2017b). Although no complete tooth has been found, we assign the Upper Pubu specimens to *Stegodon* sp.

Elephas maximus: One permanent tooth and one deciduous tooth can be clearly assigned to *Elephas*, although both are incomplete. Compared with *Stegodon*, their crowns are much higher and the lamellae are closely arranged but not connected at the base. The milk tooth (UPB494) only preserves three lamellae (Fig. 4A). The residual length of UPB494 is 32.48 mm, with a measurable maximum width of 33.26 mm. The lamellae are thinner than that of *Stegodon* teeth, with the thickness ranging from 5.36 to 6.78 mm, and the thickness of the enamel layer is only about 1.33 mm. The specimen is highly worn, and the dentine is completely exposed, forming enamel loops. The median sinus is absent. The enamel layer is extremely dense and has more regular folds. The permanent tooth (UPB502) is a left lower molar, which has a similar structure but higher crown and elongated lamellae (Fig. 4B–C). Seven and a half lamellae are preserved with the maximum remaining length of 118.85 mm, and the maximum remaining buccolingual diameter of 59.45 mm, which is located at the first preserved lamella. The lamellar frequency is 6.5 (number of plates in a standard distance of 10 cm of crown length). The morphology and metric data of the Upper Pubu specimens is close to the *Elephas maximus* fossils from Mawokou Cave and Coc Muoi (Wang et al., 2017b; Bacon et al., 2018a).

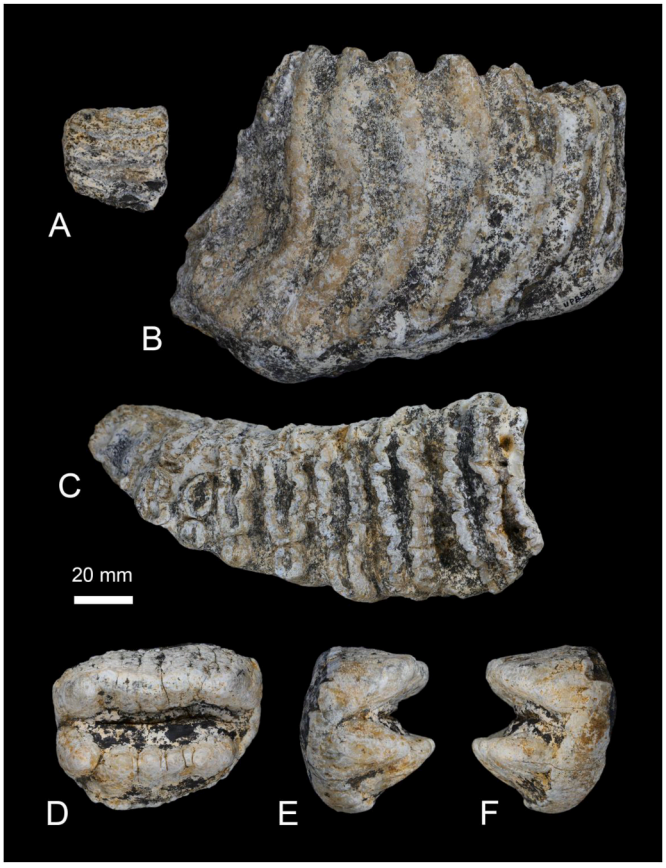

Fig. 4. Proboscidae from Upper Pubu Cave. *Elephas maximus* (A-C): A, dp (UPB494) in occlusal view; B-C, Left m (UPB502) in lingual (B) and occlusal (C) views. *Stegodon* sp. (D-F): D-F, Right M1 (UPB493) in occlusal (D), buccal (E) and lingual (F) views.

4.1.4. Carnivora

Ailuropoda melanoleuca baconi: Fourteen isolated giant panda teeth (one P2, one P3, three M3s, two M2s, one p2, one p3, one p4, two m1s and two m2s) have been identified in the Upper Pubu deposits. A fragment of a P2 with a large paracone and a well preserved metastyle is present. The outline of the P3 is narrow and long, with a distinct concavity inward between the two cusps on the lingual side (Fig. 5A). The P3 has five cusps, and the parastyle of the P3 is much more well-developed than that of the P2. The crown of the M1s is relatively low, and the occlusal outline approximates a rounded square (Fig. 5B). The lingual cingulum of the M1s is wide with many accessory tubercles. The occlusal outline of the M2s is nearly trapezoidal (Fig. 5C). The M2s have a trigon consisting of the paracone, metacone and protocone, and are characterized by a distinct talon supported by an elongated metaconule. There are many tubercles and ridges medial to the metaconule and the entometaconule is subdivided into many small cusps. A well-developed medial cingulum surrounds the mesiolingual corner of the crown. The lower premolars have similar structures with three cusps. However, the parastylid becomes stronger from p2 to p4 (Fig. 5D–E). Unlike the p2 and the p3, the parastylid and the metastylid in the p4 are on the same line as the protoconid. The m1s display a dumbbell shape with a well-developed accessory cusplet on the buccal side of the anterior region (Fig. 5F). The m2s show a rounded rectangular outline with four main cusps (Fig. 6G). Among the fossil species of giant pandas, the dental morphology and size of the Upper Pubu specimens are consistent with that of *Ailuropoda melanoleuca baconi*. Hence, we attributed the fourteen Upper Pubu specimens to *A. melanoleuca baconi* (Table S6).

Arctonyx collaris: Seven teeth conform to the dental pattern of *Arctonyx collaris* (Jiangzuo et al., 2018a), including one fragmentary m1 and six M1s. The outline of the M1s generally approximates a rhomboid shape in occlusal view (Fig. 5H). A weak ridge between the protocone and metaconule and a strong ridge between the protocone and hypocone are present on the M1s. The mesial end of the m1 specimen is partly absent, but its shape is relatively narrow and the talonid rim cusps are quite pronounced. The metric dimensions of the Upper Pubu Cave specimens are within the size range of fossils from Yixiantian Cave (Pan et al., 2023), Ganxian Cave (Liang et al., 2022), and Yangjiawan Cave 2 (Jiangzuo et al., 2018b), but bigger than those from Tham Wiman Nakin (Suraprasit et al., 2021) and Duoi U'Oi (Bacon et al., 2018b) (Table S7).

Ursus thibetanus: Altogether 36 teeth, which is the highest number among Carnivora, can be allocated to *Ursus thibetanus* given the morphology and metric dimensions of the specimens (Bacon et al., 2008; Fan et al., 2022b; Jiangzuo et al., 2018b; Liang et al., 2022; Pan et al., 2023; Suraprasit et al., 2021) (Table S8). The P4s present a subtriangular outline in occlusal view (Fig. 5I). The paracone on the buccal side is the highest and most developed cusp. The occlusal outline of the M1s is sub-rectangular, and the distal width is generally slightly larger than the mesial width (Fig. 5J). Both the parastyle and the metastyle are well developed. A cingulum is always present at the base of the buccal side of the crown, while it is weak or absent on the lingual side. The crown of the M2s is relatively low with a trapezoidal shape (Fig. 5K). The talon is significantly elongated. The cingulum is present at the base of the lingual crown in some specimens. Compared with *Ursus (Helarctos) malayanus* (Bacon et al., 2008), the m1 of *U. thibetanus* is relatively long

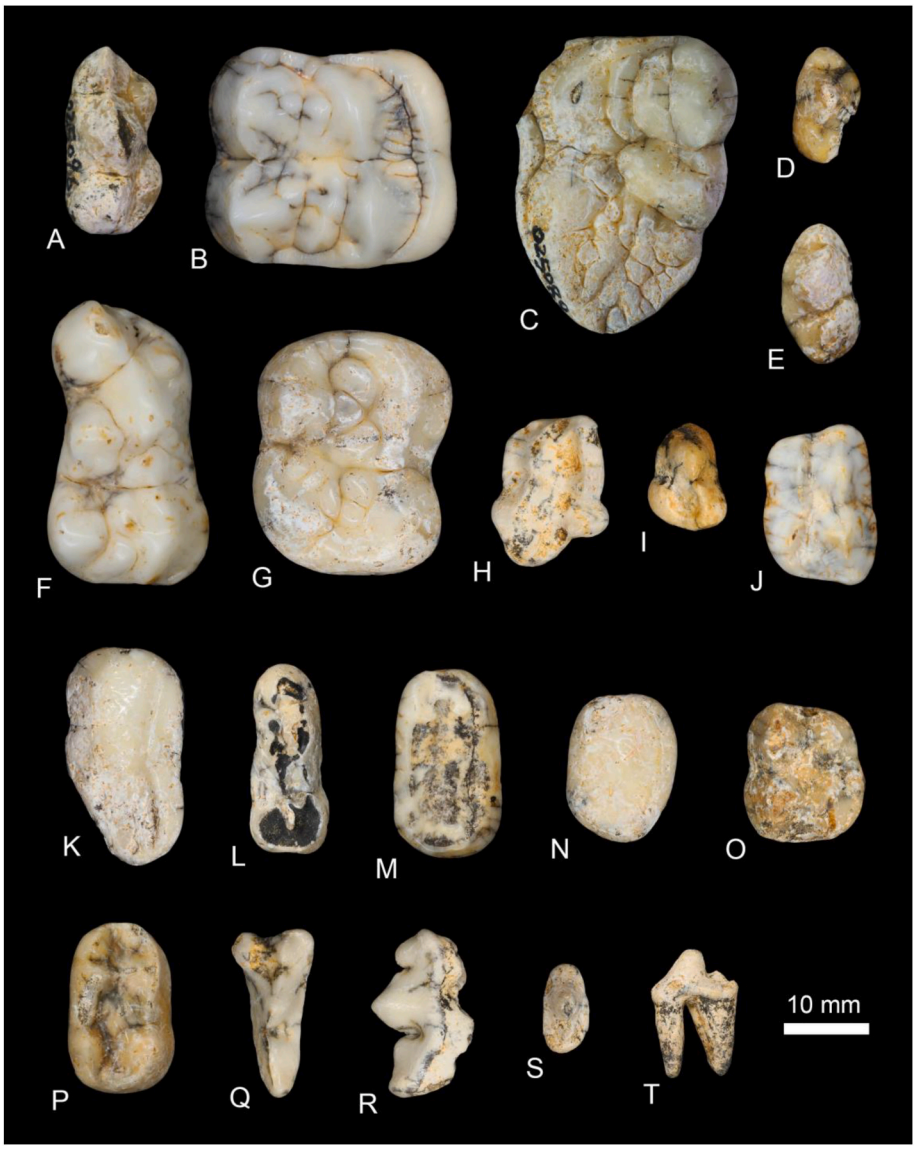

Fig. 5. Carnivora from Upper Pubu Cave. *Ailuropoda melanoleuca baconi* (A-G): A, Right P3 (025096) in occlusal view; B, Right M1 (TPB016) in occlusal view; C, Left M2 (025089) in occlusal view; D, Left p2 (TPB022) in occlusal view; E, Right p3 (025101) in occlusal view; F, Right m1 (TPB019) in occlusal view; G, Right m2 (UPB149) in occlusal view. *Arctonyx collaris* (H): H, Left M1 (UPB431) in occlusal view. *Ursus thibetanus* (I-N): I, Left P4 (TPB014) in occlusal view; J, Left M1 (TPB009) in occlusal view; K, Right M2 (UPB298) in occlusal view; L, Right m1 (UPB296) in occlusal view; M, Right m2 (UPB436) in occlusal view; N, Left m3 (UPB154) in occlusal view. *Ursus (Helarctos) malayanus* (O-P): O, Right M1 (UPB153) in occlusal view; P, Right m2 (UPB435) in occlusal view. *Neofelis nebulosa* (Q-T): Q-R, Left P4 (TPB020) in occlusal (Q) and buccal (R) views; S-T, Left p3 (UPB505) in occlusal (S) and buccal (T) views.

and narrow, with the posterior ridge of the metaconid nearly parallel to the posterior ridge of the protoconid, and its talonid is slightly wider than the trigonid (Fig. 5L). The m2 shows a rounded rectangular outline in occlusal view (Fig. 5M). A transverse ridge connects the protoconid with the metaconid, but is separated into two parts by a central valley. The occlusal surface of the m3 is nearly oval, with delicate wrinkles on it (Fig. 5N).

Ursus (Helarctos) malayanus: Six isolated teeth (four M1s and two m2s), belong to *Ursus (Helarctos) malayanus*. Compared with the teeth of *Ursus thibetanus*, those of *U. malayanus* are generally smaller and appear shorter and wider. The M1s show a nearly square occlusal surface, with well-developed lingual and buccal cingula (Fig. 5O). The parastyle and metastyle are weakly developed, which is also different from *U. thibetanus*. The crown of the m2s is relatively short and wide, not as elongated as that of *U. thibetanus*, and with inconspicuous cusp splitting (Fig. 5P). The morphology of the teeth conforms to those described in Yixiantian Cave (Pan et al., 2023), Yangjiawan Cave 2 (Jiangzuo et al., 2018b), and Tam Hang (Bacon et al., 2011), and their metric dimensions show a great deal of overlap (Table S9) (Bacon et al., 2011; Badoux, 1959; Jiangzuo et al., 2014; Pan et al., 2023; Smith et al., 2021).

Neofelis nebulosa: Two teeth (one P4 and one p3) conform to the dental pattern of the medium-sized felid *Neofelis nebulosa*. The P4, which is the most diagnostic tooth except the canine to identify the species (Jiangzuo et al., 2018b), has a relatively long and narrow crown (Fig. 5Q-R). The paracone is the highest and largest cusp. The anterior external corner of the parastyle projects towards the buccal side but the ectoparastyle is not formed. The occlusal surface of the p3 presents an oval shape, with a slightly wider posterior part (Fig. 5S-T). Both parastylid and metastylid are present, but parastylid is weakly developed. The dimensions of the Upper Pubu teeth fall within the range of fossils from Yixiantian Cave (Pan et al., 2023) and Yangjiawan Cave 2 (Jiangzuo et al., 2018b), but slightly larger than those from Mocun Cave (Fan et al., 2022b) and Duoi U'Oi Cave (Bacon et al., 2008) (Table S10).

Carnivora indet.: Two incisors of Carnivora are present, but they are

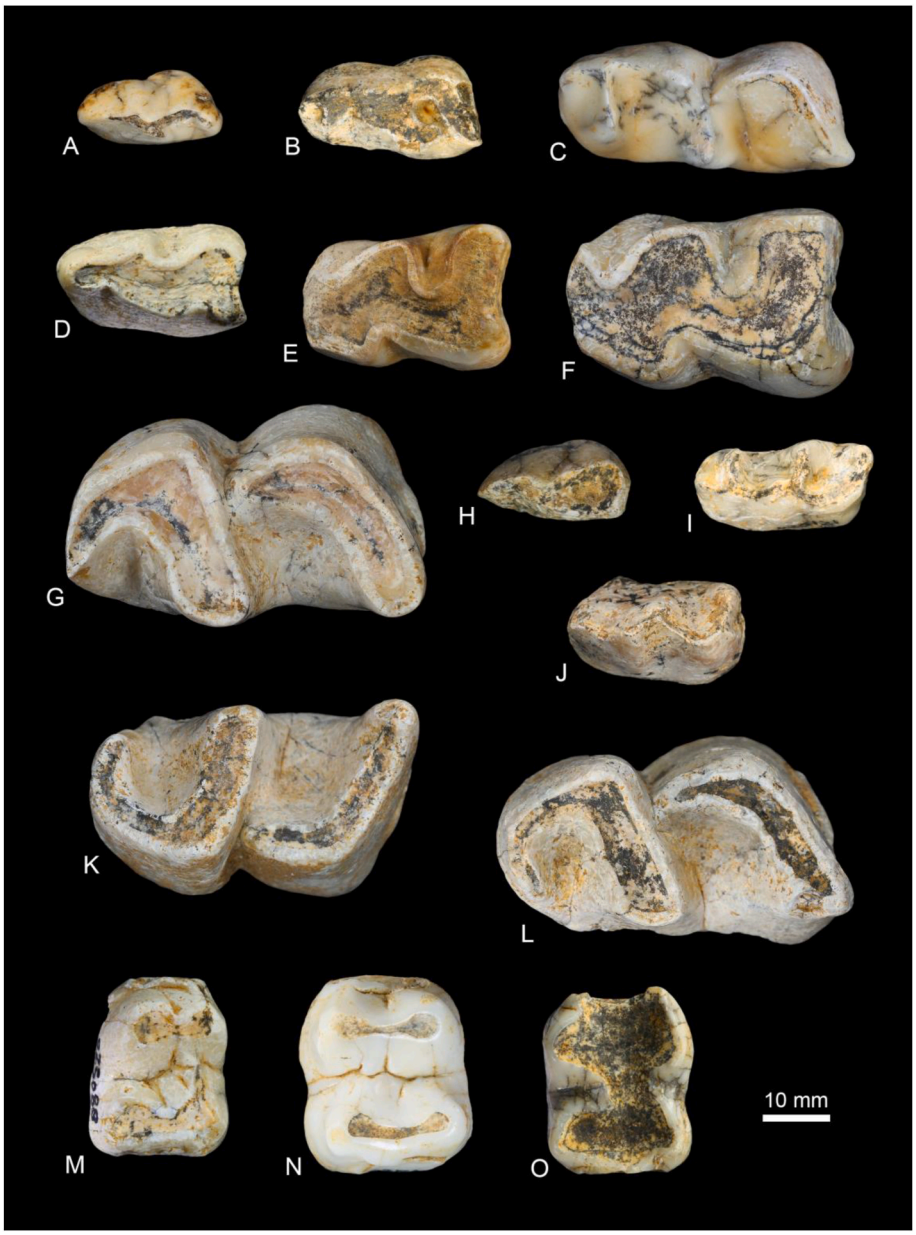

Fig. 6. Perissodactyla from Upper Pubu Cave. *Rhinoceros sondaicus* (A-G): A, Right dp1 (TPB028) in occlusal view; B, Right dp2 (025124) in occlusal view; C, Right dp3 (UPB531) in occlusal view; D, Right p2 (025120) in occlusal view; E, Left p3 (UPB522) in occlusal view; F, Left p4 (UPB529) in occlusal view; G, Right m3 (UPB527) in occlusal view. *Dicerorhinus sumatrensis* (H-L): H, Right dp1 (025122) in occlusal view; I, Left dp2 (025121) in occlusal view; J, Left p2 (UPB523) in occlusal view; K, Left m1 (UPB525) in occlusal view; L, Right m3 (UPB528). *Tapirus sinensis* (M-O): M, Right p3 (025088) in occlusal view; N, Left p4 (025105) in occlusal view; O, Right m1 (025108) in occlusal view.

unidentifiable.

4.1.5. Perissodactyla

Rhinoceros sondaicus: Ten isolated teeth, including six deciduous teeth, three premolars and 1 M are assigned to *Rhinoceros sondaicus*. The fragmentary DP2 has a well-developed posterior cingulum with a post-fossette present on the distal end of the crown. The crochet and crista join together to form a medifossette, which has three small spines on the side near the metaloph. The median valley broadly opens with no tubercular structures at the entrance. The occlusal surface of the dp1 is nearly an elongated oval, with relatively simple structure (Fig. 6A). The talonid is narrow and the posterior valley opens lingually backwards. The crown of the dp2s is trilobal in structure, slightly narrow in anterior part (Fig. 6B). The talonid is nearly closed (TPB029) or appears as a closed enamel ring (025124) when highly worn. The structure of the dp3 is similar to the dp2, but much larger in size and its anterior ectolophid groove is marked (Fig. 6C). Weak cingula are present on the dp3. The posterior valleys are V-shaped on the dp3 and p2 in lingual view. The p2 has a more developed trigonid and a shallow ectolophid groove (Fig. 6D). Both the p3 and the p4 specimens are highly worn and do not have the posterior cingulum (Fig. 6E–F). The lingual side of the metaconid on the m3 exhibits a convex shape in occlusal view (Fig. 6G). The specimens fall within the range of *R. sondaicus* in terms of metric dimensions (Table S11) and morphological features (Bacon et al., 2008, 2011, 2018a,b; Liang et al., 2022; Suraprasit et al., 2016; Yan et al., 2020).

Dicerorhinus sumatrensis: Seven lower teeth are recognized as *Dicerorhinus sumatrensis* (two dp1s, one dp2, two p2s, one m1 and one m3). The dp1s are approximately triangular in shape with a simple occlusal pattern (Fig. 6H). The paralophid is bifurcated and the anterior

ectolophid groove is marked on the dp2 (Fig. 6I). The dp2 of *D. sumatrensis* is generally narrower than that of *Rhinoceros sondaicus*. The anterior cingulum of the p2 is absent, while the posterior one is weak (Fig. 6J). On the m1 and m3, the lingual side of the metaconid appears to be flat in occlusal view (Fig. 6K-L). The dimensions of the specimens are mostly smaller and narrower than those of the Upper Pubu *R. sondaicus* (Table S11). The Upper Pubu *D. sumatrensis* fossils mostly fall within the range of samples from notably *Gigantopithecus* Cave (Tong and Guérin, 2009), and are comparable to those from Ganxian Cave (Liang et al., 2022), Coc Muoi Cave (Bacon et al., 2018a) and Duoi U'Oi Cave (Bacon et al., 2008) (Table S12).

Rhinoceros sp.: Twelve specimens are allocated to *Rhinoceros* sp., but cannot be identified to specific species due to their highly worn and fragmented nature.

Tapirus sinensis: Nine permanent teeth (one p3, four p4s, three m1s and one m2) found in Upper Pubu are attributed to the extinct tapir *Tapirus sinensis*. The occlusal surface of the p3 is trapezoidal, with a narrow anterior lobe and a wide posterior lobe (Fig. 6M). The paralophid is reduced into a cingulum, and the protolophid and the hypolophid are basically parallel to each other. The protolophid is higher but narrower than the hypolophid. The metalophid is slightly curved and connects with the hypoconid at the end. The p4s display a sub-rectangular occlusal outline, and the hypolophid is wider than the thick protolophid (Fig. 6N). The paraconid is reduced, whereas the other four main cusps are well-developed. The posterior cingulum is absent. All three m1s are highly worn, showing a sub-rectangular shape with a

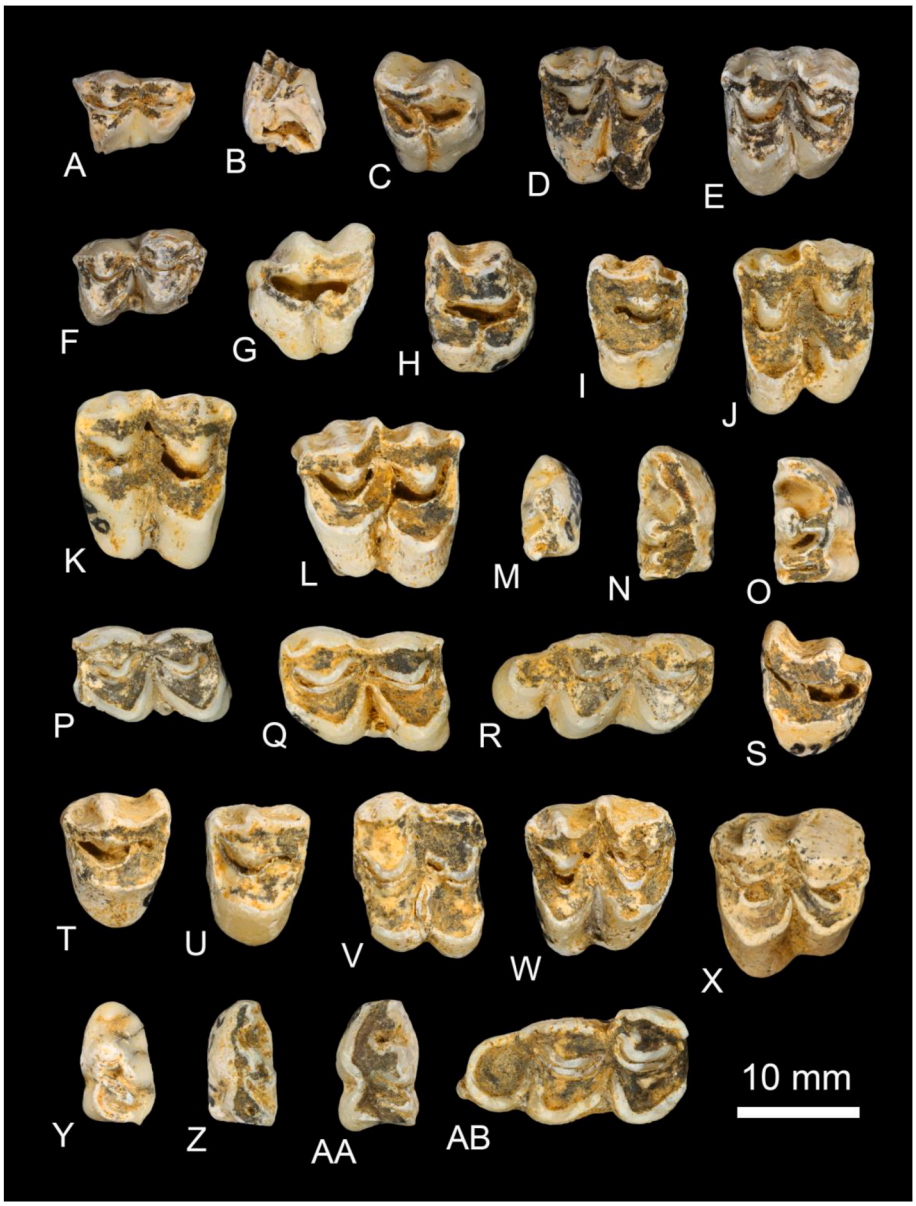

Fig. 7. Fossil teeth of *Muntiacus reevesi* (A–F), *Muntiacus muntjak* (G–R), and *Elaphodus cephalophus* (S-AB) from Upper Pubu Cave. *Muntiacus reevesi* (A-F): A-B, Right dp4 (UPB134) in occlusal (A) and distal (B) views; C, Right P2 (UPB432) in occlusal view; D, Right M2 (UPB129) in occlusal view; E, Left M3 (UPB133) in occlusal view; F, Right m2 (UPB214) in occlusal view. *Muntiacus muntjak* (G-R): G, Left P2 (024920) in occlusal view; H, Right P3 (025830) in occlusal view; I, Right P4 (025714) in occlusal view; J, Left M1 (025673) in occlusal view; K, Right M2 (025590) in occlusal view; L, Right M3 (024853) in occlusal view; M, Right p2 (025884) in occlusal view; N, Right p3 (024953) in occlusal view; O, Right p4 (024954) in occlusal view; P, Left m1 (024860) in occlusal view; Q, Left m2 (024898) in occlusal view; R, Right m3 (024876) in occlusal view. *Elaphodus cephalophus* (S-AB): S, Right P2 (025843) in occlusal view; T, Left P3 (025761) in occlusal view; U, Left P4 (025766) in occlusal view; V, Right M1 (024971) in occlusal view; W, Left M2 (025783) in occlusal view; X, Left M3 (024848) in occlusal view; Y, Left p2 (024960) in occlusal view; Z, Left p3 (025861) in occlusal view; AA, Left p4 (024955) in occlusal view; AB, Right m3 (025776) in occlusal view.

slightly larger anterior width (Fig. 6O). Both the anterior and the posterior cingula are present, and there is no crista between the metalophid and the hypolophid. The structure of the highly worn fragmentary m2 specimen is similar to the m1s but the protolophid is even wider. The morphology and dimensions of the Upper Pubu teeth conform to *T. sinensis* from Longgudong (Tong, 2004, 2005), Ganxian Cave (Liang et al., 2022), and Mocun Cave (Fan et al., 2022b) (Table S13).

4.1.6. Artiodactyla

Muntiacus reevesi: Five isolated teeth (one dp4, one P2, one M2, one M3 and one m2) belong to the small-sized cervid, *Muntiacus reevesi*. The dp4 specimen (UPB134) is fragmentary and the third lobe is not preserved (Fig. 7A–B). The parastylid is quite robust while the ribs are weakly developed. The P2 shows a trapezoidal occlusal outline, with a relatively weak parastyle, robust metastyle and a paracone rib (Fig. 7C). The entoflexus is prominent, separating the protocone and metaconule. The medial crista is present whereas the cingulum is absent. The occlusal outlines of the M2 and M3 are square with four cusps, and the entostyle is weak on the M2 and absent on the M3. The dental structure of the M3 is similar to the M2, but the second lobe is obviously contracted and the metastyle is weaker (Fig. 7D–E). The cingulum is weakly developed or absent, the neocrista and spur of these two teeth are absent. The outline of the m2 is rectangular in occlusal view (Fig. 7F). It has well-developed parastylid, metastylid, entostylid and anterior cingulum. *M. reevesi* resemble *Muntiacus muntjak* in dental morphology, but is smaller in size. The dimensions of the Upper Pubu teeth, despite the slightly larger width of the P2, fall within the range of *M. reevesi* from Yixiantian Cave (Pan et al., 2023), Ganxian Cave (Liang et al., 2022), Yangjiawan and Fuyan Caves (Zhang et al., 2018a,b) and Mocun Cave (Fan et al., 2022b) (Table S14).

Muntiacus muntjak: The larger *Muntiacus* is represented by 230 specimens, including 3 upper deciduous teeth, 92 permanent premolars, and 135 M. The occlusal surface of the DP2s is trapezoidal in shape. The parastyle is relatively prominent, and the metastyle and pillars are well-developed. Both the DP2s and the DP3 have the entoflexus on the lingual side. The parastyle, mesostyle, metastyle and pillars of the DP3 are all robust, and a spur and anterior cingulum are present as well. The entoflexuses of the upper premolars identified as P2 and P3 are distinct (Fig. 7G–H). The P4s are narrower than the P3s with a weakly developed entoflexus (Fig. 7I). The upper molars display square occlusal outlines with four crescentic cusps (Figure J–L). The entostyles are always present whereas the cingulums are absent on most specimens. The metacone ribs of the upper molar are quite distinct compared to those of *Elaphodus cephalophus*. The p2s have a simple structure and its paraflexid is absent (Fig. 7M). The p3s are more robust and complex in morphology than the p2s (Fig. 7N). The metaconid is separated from the paraconid on the p4s (Fig. 7O), which makes it a “primitive” type (Zhang et al., 2018a). The m1s and m2s are composed of two lobes while the m3 is composed of three lobes (Fig. 7P-R). Though the m1s are similar to the m2s in structure, they can still be distinguished from the m2s by consistently having more worn and less developed precingulid and ectostylid. These dental patterns conform to *M. muntjak* described in Yangjiawan and Fuyan Cave (Zhang et al., 2018a), Yixiantian Cave (Pan et al., 2023), and the metric dimensions overlap those in Ganxian Cave (Liang et al., 2022), Mocun Cave (Fan et al., 2022b) and Duoi U’Oi Cave (Bacon et al., 2008) (Table S15).

Elaphodus cephalophus: 104 permanent premolars and molars, belonging to another small-sized cervid are assigned to *Elaphodus cephalophus*. Compared with *Muntiacus muntjak*, *E. cephalophus* does not have an entoflexus on the lingual side of the upper premolars. The crown of the P2s has a triangular occlusal outline without cingulum (Fig. 7S). The parastyle is relatively weaker than the metastyle. The P3s show a trapezoidal occlusal surface with longer width (Fig. 7T). Their parastyle is more developed than that of the P2s, but their metastyle and the paracone rib are less prominent. The P4s are mesiodistally shorter than the P3s (Fig. 7U). None of the upper premolars from Upper Pubu have a cingulum while most of them have developed medial cristae. The mesostyle is well-developed, the metacone rib is absent or weakly developed on the upper molars, and there is variation in the development of the entostyle (Fig. 7V–X). The paraflexid is absent and the hypoflexid is weakly developed on the p2s (Fig. 7Y). The parastylid and paraconid of the p3s are slightly forked (Fig. 7Z). The trigonid basin of the p4s is closed or nearly closed due to the metaconid being fused or almost fused with the paraconid, which represents an “advanced” type (Fig. 7AA). The mesostylid of the m1s is prominent while the metastylid is weak. The m3s of *E. cephalophus* have a larger third lobe than those of *M. muntjak* (Fig. 7AB). The morphological characteristics and dimensions of the Upper Pubu specimens are consistent with those of Yixiantian Cave (Pan et al., 2023), Yangjiawan and Fuyan Caves (Zhang et al., 2018a) (Table S16).

Cervus (Rusa) unicolor: 911 well-preserved and fragmentary teeth are attributed to *Cervus (Rusa) unicolor*, distinguished from other species of cervids from Upper Pubu by its large size. The dp3s have a comparatively thin enamel layer (Fig. 8A), while the permanent cheek teeth are covered by a thick enamel layer with a wrinkled surface that is large and robust. The protocone and hypocone of the P2s and P3s are clearly separated by the developed entoflexus on the lingual side (Fig. 8B–C). The P4s exhibit a rectangular shape in occlusal view (Fig. 8D–E), and the parastyle and the metastyle is weaker than those on the P2s and P3s. A robust and tapered entostyle is present on the lingual side of the upper molars (Fig. 8F–H). The paraflexid is absent on the p2s (Fig. 8I). The p3s have a more complicated dental pattern (Fig. 8J). The p4 specimens present two typical morphological types: one shows the fusion of the metaconid and paraconid (Fig. 8K), but the other does not (Fig. 8L). The *Palaeomeryx* fold is lacking on the lower molars (Fig. 8M-O). The dimensions of the Upper Pubu teeth largely overlap with fossil specimens from Yanlidong Cave (Yao et al., 2023), Yixiantian Cave (Pan et al., 2023), Ganxian Cave (Liang et al., 2022), Mocun Cave (Fan et al., 2022b) and Duoi U’Oi (Bacon et al., 2008) (Table S17).

Cervidae gen. et sp. indet. In addition, 7 fragmented teeth could not be accurately identified.

Sus scrofa: Suids are represented by 868 isolated teeth and tooth fragments, including 5 incisors, 2 canines, 463 premolars (Fig. 9B–D, H-J), 393 M, and 5 milk teeth (Fig. 9A). The cross-section of the only fragmented male lower canine displays the scrofic type (Sun et al., 2021a), with the narrowest labial face. Other teeth exhibit typical morphologies found in *Sus scrofa*, such as numerous accessory small tubercles on the main cusps and cuspids of the molars (Fig. 9 E-G, K-M), specifically on the m3s and M3s (Suraprasit et al., 2016; Bacon et al., 2018a). The species is recorded in South China since the Middle Pleistocene (Fan et al., 2022b; Liang et al., 2022; Rink et al., 2008; Wang et al., 2007). The range of the dimensions also largely overlap that of *S. scrofa* from the sites Yenchingkuo (Colbert and Hooijer, 1953), Ganxian Cave (Liang et al., 2022), Mocun Cave (Fan et al., 2022b) in South China, Tham Wiman Nakin in Northeast Thailand (Suraprasit et al., 2021) and Duoi U’Oi Cave in northern Vietnam (Bacon et al., 2008) (Table S18).

Capricornis sumatraensis: 23 isolated permanent teeth are assigned to *Capricornis sumatraensis*. All of the specimens have smooth enamel surfaces. The styles and stylids are robust. The P3s have a semicircular occlusal outline with a well-developed parastyle and metastyle, and a quite distinct paracone rib (Fig. 9N). No entoflexus is present on the lingual side. Both the M1 and M3 are composed of two lobes. The mesostyle of the M1 is more prominent than the parastyle and metastyle (Fig. 9O). The M3 has a more contracted second lobe (Fig. 9P-Q). On the upper molars, the ribs are weakly developed, and the cingulum and the entostyle are absent. The mesial fossette is present on the occlusal surface when the upper molars are moderately worn. The p4s display clear molarization (Fig. 9R). No ectostylid and cingulum appear on the m1 (Fig. 9S-T) and m3s (Fig. 9V). The m2s are more robust than the m1 (Fig. 9U). The morphology and dimensions of the specimens are consistent with those described in Yixiantian Cave (Pan et al., 2023),

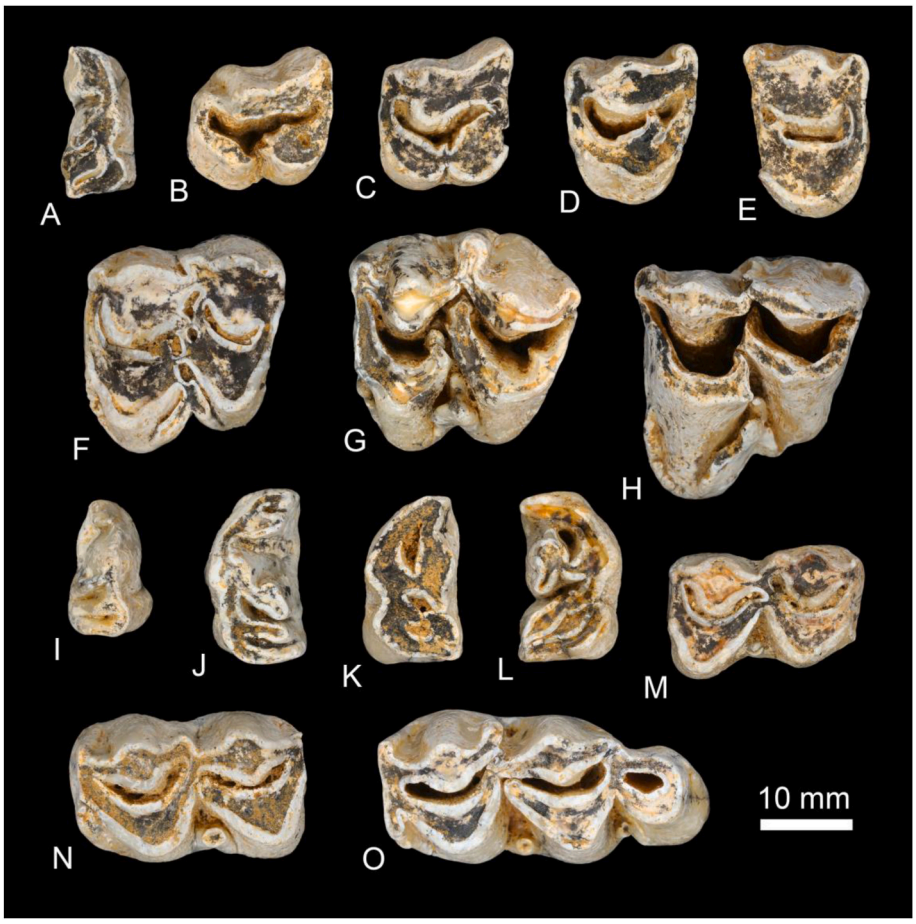

Fig. 8. Fossil teeth of *Cervus (Rusa) unicolor* from Upper Pubu Cave. A, Right dp3 (UPB108) in occlusal view; B, Left P2 (UPB082) in occlusal view; C, Left P3 (UPB085) in occlusal view; D, Left P4 (UPB084) in occlusal view; E, Right P4 (UPB159) in occlusal view; F, Left M1 (UPB162) in occlusal view; G, Left M2 (UPB074) in occlusal view; H, Left M3 (UPB070) in occlusal view; I, Right p2 (UPB102) in occlusal view; J, Left p3 (UPB064) in occlusal view; K, Left p4 (UPB060) in occlusal view; L, Right p4 (UPB063) in occlusal view; M, Right m1 (UPB180) in occlusal view; N, Left m2 (UPB086) in occlusal view; O, Left m3 (UPB175) in occlusal view.

Ganxian Cave (Liang et al., 2022), Tham Wiman Nakin (Suraprasit et al., 2021) and Duoi U'Oi Cave (Bacon et al., 2008) (Table S19).

Bos gaurus: 43 teeth can be assigned to *Bos gaurus*. The majority of the specimens are highly worn or fragmentary. The P4s display compressed but well-developed parastyles and metastyles, and a complex fossette shape (Fig. 9W). The only upper molar specimen is moderately worn, showing a rectangular occlusal outline, with a well-developed mesostyle and bifurcated entostyle (Fig. 9X-Y). The two p2s are highly worn and the posterior fossette is present (Fig. 9Z). The p3s exhibit a larger postprotocristid and a poorly developed premetacristid than the p4s (Fig. 9AA-AB). The p4s have a narrow postprotocristid which constricts anteroposteriorly and a prominently developed metaconid (Fig. 9 AC-AD). The lower molars display slightly developed ectostylids without furcation (Fig. 9AE-AG). Along with the consistency of morphological characters, the size of the Upper Pubu *B. gaurus* specimens also falls within the range of the Yixiantian, Ganxian, Khok Sung and Tham Wiman Nakin fossil assemblages (Liang et al., 2022; Pan et al., 2023; Suraprasit et al., 2016, 2021) (Table S20).

5. Discussion

5.1. Composition of the Upper Pubu fauna and its position in the evolutionary sequence

The Upper Pubu mammalian assemblage consists of 24 identified taxa (14 families, 20 genera) from six orders (Primates, Carnivora, Proboscidea, Perissodactyla, Artiodactyla, and Rodentia) (Fig. 10, Table 2). Artiodactyla (Cervidae, Bovidae, Suidae) are extremely dominant in the faunal assemblage (91.4% according to NISP and 76.6% according to MNI). On the contrary, Primates make up a very limited proportion of the fauna (1.1% based on NISP and 3.3% based on MNI). Only three globally extinct taxa (*Ailuropoda melanoleuca baconi*, *Stegodon* sp., *Tapirus sinensis*) are recorded in the Upper Pubu Cave. Seven other taxa, including *Pongo* sp., *Elephas maximus*, *Ursus (Helarctos) malayanus*, *Capricornis sumatraensis*, and three types of rhinoceros (*Rhinoceros sondaicus*, *Dicerorhinus sumatrensis*, *Rhinoceros* sp.) went locally extinct, but continues to survive in present-day Southeast or South Asia.

The composition of the Upper Pubu fauna is slightly less diverse in terms of the number of genera than that of the Ganxian fauna, which is of a slightly earlier age in the same region, but more diverse than that of the Baolai fauna, which has a later Pleistocene age (Table 3). Compared with the contemporaneous Baxian fauna and the earlier Yixiantian fauna in the Chongzuo region, the species diversity of the Upper Pubu fauna is significantly lower, especially regarding carnivores (Table 3). Many species of Carnivora (*Cuon*, *Paguma*, *Mustela*, *Martes*, *Melogale*, *Lutra*, *Herpestes*, *Crocuta*, etc.) are not found in the Upper Pubu faunal collection.

In addition, the Baxian fauna has a high degree of similarity and inheritance in species composition with the chronologically older Yixiantian fauna that is from the same region (Pan et al., 2023; Zhang et al., 2024). The discovery of one specimen of *Gigantopithecus blacki* in the Yixiantian Cave mammalian assemblage, along with its absence in the late Middle Pleistocene Baxian Cave fauna, demonstrates the pre-extinction stage and post-extinction stage in the evolutionary

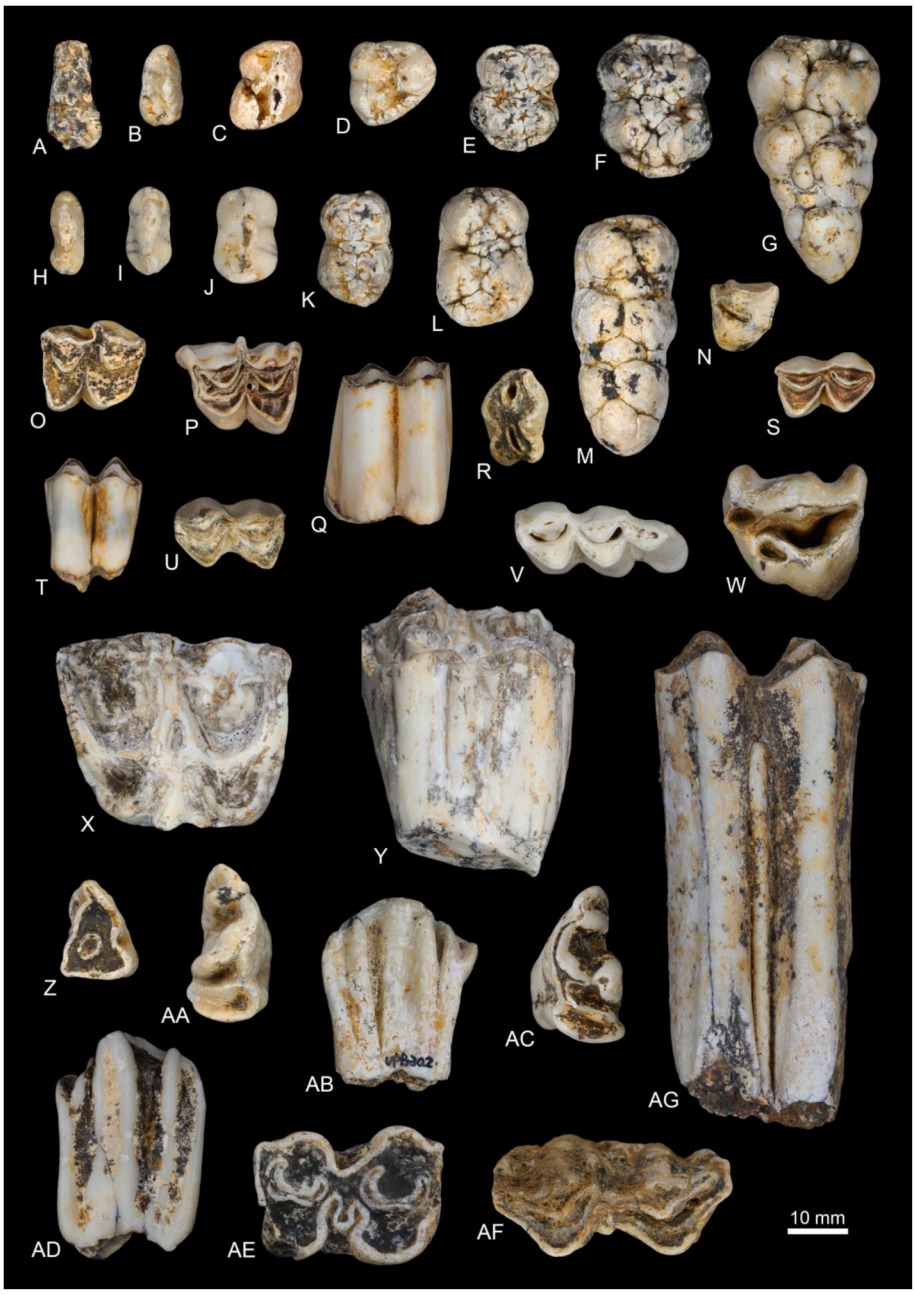

Fig. 9. Fossil teeth of *Sus scrofa* (A–M), *Capricornis sumatraensis* (N–V), and *Bos gaurus* (W-AF) from Upper Pubu Cave. *Sus scrofa* (A-M): A, Right dp4 (UPB057) in occlusal view; B, Left P2 (UPB049) in occlusal view; C, Left P3 (UPB256) in occlusal view; D, Right P4 (UPB031) in occlusal view; E, LM1 (UPB026) in occlusal view; F, Right M2(UPB013) in occlusal view; G, Right M3 (UPB232) in occlusal view; H, Left p2 (UPB053) in occlusal view; I, Right p3 (UPB285) in occlusal view; J, Left p4 (UPB276) in occlusal view; K, Left m1 (UPB023) in occlusal view; L, Right m2 (UPB018) in occlusal view; M, Right m3 (UPB003) in occlusal view. *Capricornis sumatraensis* (N-V): N, Left P3 (024857) in occlusal view; O, Left M1 (UPB139) in occlusal view; P-Q, Right M3 (TPB044) in occlusal (P) and lingual (Q) views; R, Left p4 (025077) in occlusal view; S-T, Right m1 (TPB031) in occlusal (S) and buccal (T) views; U, Left m2 (025060) in occlusal view; V, Left m3 (TPB032) in occlusal view. *Bos gaurus* (W-AF): W, Right P4 (UPB324) in occlusal view; X-Y, Right M1/2 (TPB065) in occlusal (X) and lingual (Y) views; Z, Right p2 (UPB535) in occlusal view; AA-AB, Right p3 (UPB302) in occlusal (AA) and lingual (AB) views; AC-AD, Left p4 (TPB061) in occlusal (AC) and lingual (AD) views; AE, Right m1 (UPB304) in occlusal view; AF-AG, Left m2 (UPB141) in occlusal (AF) and buccal (AG) views.

history of *G. blacki*, respectively (Zhang et al., 2024). However, no *G. blacki* fossils were identified in Ganxian Cave or Upper Pubu Cave, which also coincides with the time of its extinction in the Chongzuo area.

Megatapirus augustus, not *Tapirus sinensis*, is present in both the Yianxiantian and Baxian Cave faunas, whereas these two species coexist in the penecontemporaneous Wuyun Cave and Ganxian Cave faunas located in the Bubing Basin (Chen et al., 2002; Liang et al., 2022). However, only *T. sinensis* is present in the Upper Pubu Cave, and the situation of the Diaozhongyan fauna in northeast Guangxi is consistent with that of Upper Pubu (Liang et al., 2020), while *M. augustus* alone is seen in the Late Pleistocene Fuyan Cave in Hunan (Li et al., 2013). Given that *M. augustus* was found to have replaced *T. sinensis* in the well-defined stratigraphic accumulations of the Late Pleistocene Mocun Cave (Fan et al., 2022b), the variation in the presence or absence of these two species in the faunas from various cave sites during the Middle Pleistocene may simply be a regional distributional difference that does not reflect a broader replacement trend.

Despite marking the transition between the Middle and Late

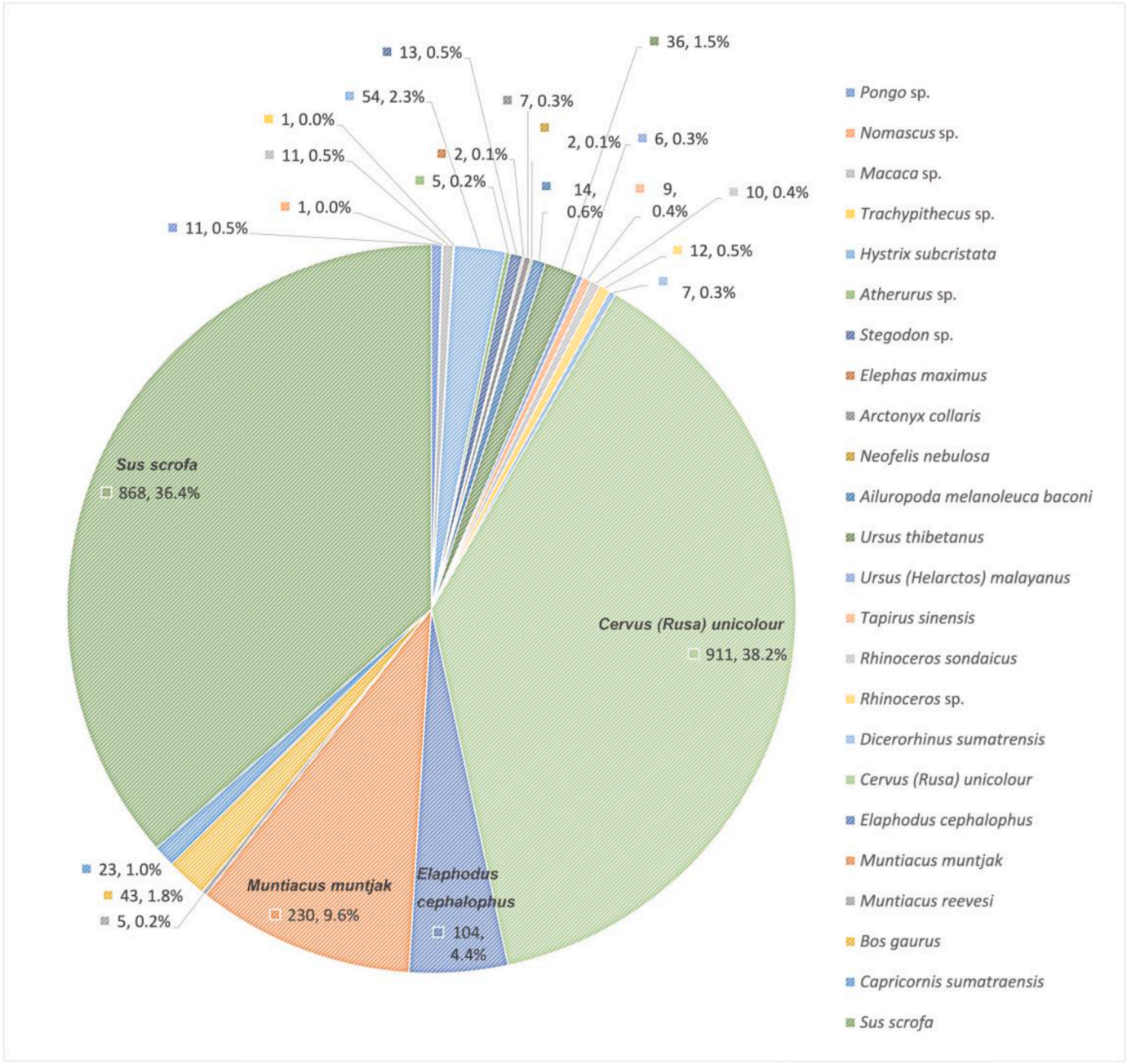

Fig. 10. The faunal composition of Upper Pubu based on the NISPs of identified taxa.

Pleistocene, Upper Pubu exhibits a faunal composition largely similar to that of the Late Pleistocene faunas in Fuyan Cave, Mocun Cave, and Baolai Cave, with typical species of the *Stegodon-Ailuropoda* fauna in South China still present. However, the Upper Pubu fauna shows a relatively larger proportion of globally or locally extinct (no longer survive in Guangxi province or southern China) medium and large sized mammal species (41.7%), which is slightly higher than that of the Mocun fauna (38.5%), notably surpassing that of the Fuyan fauna (32.1%) and the Baolai fauna (30.0%).

This observation also highlights the value of intra-regional faunal comparisons as the result is more illuminating. Interestingly, in the Bubing Basin, this proportion progressively declines in chronological order, from 53.6% for the Ganxian fauna, through 47.8% for the Wuyun fauna, 41.7% for the Upper Pubu fauna, 30.0% for the Baolai fauna, and finally to the Cunkong fauna at 20% (Fig. 11). It is evident that from the Middle to the Late Pleistocene and then to the Holocene, extinct elements in the mammalian faunas in South China were gradually eliminated, while extant ones thrived. As shown, this change in ratio can provide insights into the biochronological sequence of the faunas, at least within the local biocenosis (Fig. 11). As a result, in cases where accurate radiometric dating of a particular fauna is absent, a more precise judgment can still be made regarding its position in the evolutionary sequence based on the proportion of extinct taxa.

Overall, the Upper Pubu fauna exhibits typical features of a late Middle Pleistocene mammalian assemblage from the region. The biochronological age of Upper Pubu is consistent with the radiometric ages obtained using U-series, ESR, and OSL dating methods (Rink et al., 2008; Zhang et al., 2024). Furthermore, Upper Pubu displays a greater degree of modernity in faunal composition than Wuyun (Wang et al., 2007), Ganxian (Liang et al., 2022), Yixiantian (Pan et al., 2023), and Diaozhongyan (Liang et al., 2020; Liao et al., 2020); all cave localities that are older in age than Upper Pubu (Table 3).

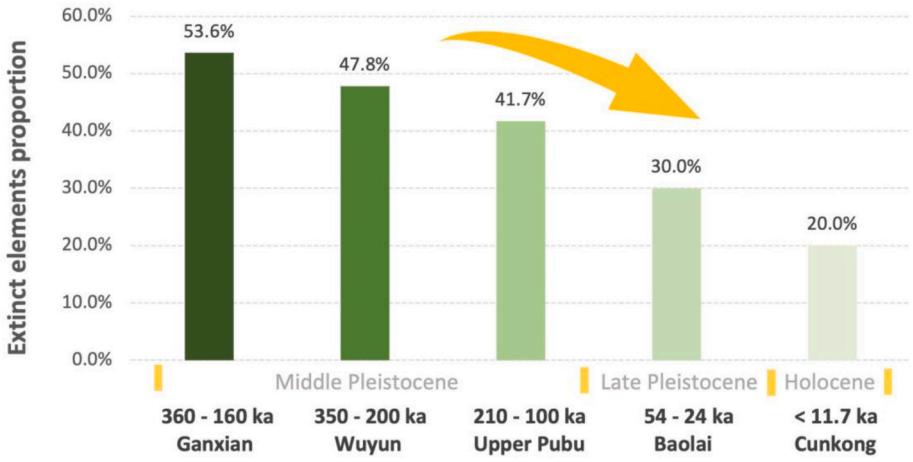

Fig. 11. The change in the proportion of extinct elements (including global and local) from the Middle Pleistocene to Holocene faunas in the Bubing Basin. This change is evident in five cave sites: Ganxian Cave (Liang et al., 2022), Wuyun Cave (Chen et al., 2002), Upper Pubu Cave, Baolai Cave (Fan et al., 2022a), and Cunkong Cave (Wang et al., 2007).

Compared with Late Pleistocene fossil assemblages in the region, Upper Pubu is comparable to Fuyan (Li et al., 2013), Mocun (Fan et al., 2022b), and Baolai (Fan et al., 2022a) in terms of the proportion of extinct species (Table 3). Thus, the similarity between the faunas of the two periods (late Middle Pleistocene: Upper Pubu; Late Pleistocene: Fuyan; Mocun; Baolai) indicates a transition towards extant faunas that began by the terminal Middle Pleistocene in southern China. On the other hand, the faunas in southeast Asia seem to retain less archaic elements throughout the period, which can be observed from Coc Muoi, Duoi U'Oi and Ma U'Oi Caves in northern Vietnam (Bacon et al. 2008, 2018a, 2018b), Ngalau Gupin Cave in Sumatra (Smith et al., 2021), Punung in Java (Badoux, 1959; Storm and de Vos, 2006), and Nam Lot Cave in northern Laos (Bacon et al., 2018b).

5.2. Comparison of the Upper Pubu, Ganxian, and Baxian faunas: insights into Stegodon-Ailuropoda variation

Here we compare the composition of the Upper Pubu fauna with two penecontemporary sites, Ganxian Cave, which is also located in the Bubing Basin, and Baxian Cave, situated in the Chongzuo region (Table 4). The age range of Ganxian is from 362 ± 78 ka to 168.9 ± 2.4 ka (Liang et al., 2022), slightly older than that of Upper Pubu, while the age of Baxian is constrained between 232 ka to 129 ka (Zhang et al., 2024). The comparison of these three collections is important for understanding the characteristics of the mammalian faunas at the transition of the Middle to Late Pleistocene in the Bubing Basin, and also for identifying faunal differences across the two regions, revealing variation in the *Stegodon-Ailuropoda* Faunal Complex in southern China.

In the late Middle Pleistocene, *Gigantopithecus* became completely extinct and was not found in any of the three caves. In Primates, Cercopithecidae has the largest number of species present in all three faunas. As for Hominidae, the Ganxian and the Upper Pubu faunas are comparable, which has only one taxon, *Pongo*, while five *Homo* teeth were discovered in the Baxian fauna. In the two caves from the Bubing Basin, the proportion of *Pongo* and *Macaca* among the Primates are similar. On the contrary, the number of *Macaca* surpasses that of *Pongo* in the Baxian Cave fauna from the Chongzuo area (Zhang et al., 2024). Hylobatidae is the least abundant family in Primates in the three assemblages. The number of Primates in Upper Pubu decreased dramatically compared to those of Ganxian and Baxian, which constituted merely 1.1% of all studied material, while Primates represented 9.2% of Ganxian and 14.5% of Baxian (still a noticeable decline when the comparision is based on MNI). Although the overall NISPs are similar (Table 4), the absolute quantity of *Pongo* and *Macaca* fossils in Ganxian is nearly nine times higher than that of Upper Pubu. Additionally, the MNI of Primates in Ganxian is also three time greater than that of Upper Pubu. Combined with the dating results of the two faunas, it may indicate that the forest area shrank and the environment deteriorated toward the end of the Middle Pleistocene (Cheng et al., 2016). Considering the higher percentage of Primates in the Baxian fauna compared to the Ganxian and Upper Pubu faunas, differences in the local paleoenvironment between the Bubing Basin and the Chongzuo area were revealed during the late Middle Pleistocene.

There are 59 specimens of Hystricidae in Rodentia, consisting of *Atherurus* sp. and *Hystrix subcristata*, representing only about 4.2% of individuals in the Upper Pubu fauna (Table 4). The proportion of Rodentia, as indicated by MNI, in Upper Pubu is far less than that of Ganxian (13.8%). As shown in Table 4, NISP% is not noticeably different from MNI% regarding Rodentia in Upper Pubu and Ganxian. Therefore, it can be estimated that the percentage of rodents in Baxian also surpasses that in Upper Pubu but is comparable to that in Ganxian.

The composition of the Proboscidea has changed considerably over time. During the Middle Pleistocene, *Sinomastodon* was no longer seen at sites within the Bubing Basin or the Chongzuo area, whereas *Elephas* appeared, with recent research showing that the earliest known Asian elephants were documented at Ganxian (Liang et al., 2022). In Upper Pubu, the remains of Elephantidae were also found. All three faunas still have relatively small percentages of Proboscidea based on total sample sizes (Table 4). It has been proposed that the shift from *Stegodon* to *Elephas* is a key for distinguishing the Middle Pleistocene faunal association of *Stegodon-Ailuropoda* from the Late Pleistocene faunal association of *Elephas-Megatapirus* (Jin et al., 2009a; Li et al., 2013). These findings suggest that Asian elephants have been present in southern China since the late Middle Pleistocene and represent a certain proportion of the faunas. During this time period, *Elephas* and *Stegodon* coexisted in southern China. Due to the small sample sizes, the slight difference in the proportion of *Elephas* and *Stegodon* at the Ganxian (0.7% and 0.4%, respectively, based on MNI) and Upper Pubu (0.8% and 0.4%, respectively, based on MNI) may only represent a change in distribution area and does not reflect a pattern of replacement. However, among the 224 specimens of Proboscidea in the Baxian fauna, the NISP of Elephantidae is nearly four times that of Stegodontidae, which may indicate a gradual replacement.

Carnivore species are diverse in all three caves, with the Baxian fauna exhibiting the highest diversity of Carnivora (Tables 3 and 4). Ursidae stands out as the most abundant family within Carnivora, dominating Upper Pubu, Baxian and Ganxian. The coexistence of *Ursus thibetanus* and *Ursus (Helarctos) malayanus* is found in Upper Pubu,

which has not been reported in other cave sites in the Bubing Basin. In comparison, Upper Pubu has a lower number of carnivorous species, notably lacking Canidae and Hyaenidae (Tables 3 and 4). The reduction of diversity in Carnivora, from 25.0% in Ganxian to 20.8% in Upper Pubu, probably suggests a deterioration in the ecological conditions in the Bubing Basin from the late Middle Pleistocene to the end of the Middle Pleistocene period. Changes in habitat environment perhaps affect the diversity of Carnivora species. Higher diversity of Carnivora in the Chongzuo Region than that of the Bubing Basin indicates different environmental context during the late Middle Pleistocene in the two areas. Further studies such as stable carbon and oxygen isotope analysis will test this hypothesis.

The Perissodactyla composition in Upper Pubu is similar to Ganxian and Baxian, except that *Megatapirus augustus* is not present in Upper Pubu (Table 3). Perissodactyla accounts for a small proportion in the three faunas, all less than 3% of the total specimens, and not much higher based on MNIs. Comparatively, there are more fossils belonging to the Rhinocerotidae than the Tapiridae. *Rhinoceros sondaicus* and *Dicerorhinus sumatrensis* are present in both Upper Pubu and Ganxian, a coexistence of these two species not previously reported in other cave sites in southern China. The increasing reports of *R. sondaicus* and *D. sumatrensis* fossils in Pleistocene strata in southern China (Liang et al., 2022; Tong and Guérin, 2009; Yan et al., 2020), along with the identification of a new species, *Rhinoceros fusuiensis* sp. nov. (Yan et al., 2014), suggests there is a need to re-evaluate previous definitions of *Rhinoceros sinensis*. Furthermore, the discovery of a gradual replacement of *Tapirus sinensis* by *M. augustus* during the Late Pleistocene in Mocun Cave (Fan et al., 2022b), and the coexistence of *T. sinensis* and *M. augustus* in Wuyun Cave and Ganxian Cave (Wang et al., 2007; Liang et al., 2022) suggests the evolutionary history of Perissodactyla was more complicated in the region.

Artiodactyla is the most abundant group in all three faunas, comprising a significant percentage of the total assemblages (Table 4). In Upper Pubu, Artiodactyla represents as much as 76.6% of individuals in the fauna, while it accounts for 58.7% in Ganxian. The composition of Artiodactyla remains stable in both Upper Pubu and Ganxian, with Cervidae being the most abundant family, followed by Suidae, which makes up around half the number of Cervidae. Bovidae, on the other hand, is limited in number, representing less than 13% of individuals in the Artiodactyla. The ratio of Cervidae to Suidae (about 1.96 in Upper Pubu and 2.48 in Ganxian based on MNI) in the Bubing Basin is completely different from that of Baxian in Chongzuo during the same period (Zhang et al., 2024). Besides, there is also a significant difference in the proportion of Bovidae between the sites in these two regions. Moreover, the presence of *Megalovis guangxiensis* exclusively in Ganxian, without any occurrences in Upper Pubu or the Late Pleistocene site of Baolai (Fan et al., 2022a), indicates its local extinction by the end of the Middle Pleistocene.

On the whole, species diversity decreased in Upper Pubu compared to Ganxian and Baxian. This decrease is particularly pronounced in Carnivora, where Canidae, Herpestidae, Hyaenidae and Viverridae are absent. Moreover, the number and proportion of Primates in Upper Pubu declined substantially. Nevertheless, Artiodactyla are absolutely dominant in Upper Pubu, representing 91.4% of the total NISP and 76.6% of the total MNI. These changes are perhaps partly due to the climatic fluctuations at the transition of the Middle and Late Pleistocene, and these other taxa are more influenced by sudden climatic changes than the Artiodactyla.

5.3. Paleoenvironmental implications

Upper Pubu can be considered a representative terminal Middle Pleistocene fauna and an informative source for analyzing ecological diversity and the paleoenvironment of the surrounding area. The presence of primate species like *Pongo* sp., *Macaca* sp., *Nomascus* sp., and *Trachypithecus* sp., is indicative of a hot and humid forested habitat (Tougard and Montuire, 2006). However, the considerable decline in the number and proportion of Primates in Upper Pubu suggests possible environmental degradation and forest reduction during the end of the Middle Pleistocene. Nonetheless, the continued presence of *Pongo* indicates that the southern part of the Bubing Basin still maintained subtropical or tropical conditions around 210–100 ka.

The extant species *Ursus (Helarctos) malayanus,* a non-hibernating omnivore who primarily inhabits dense forest areas, is well-adapted to tropical, subtropical and monsoon rainforests. China is a marginal distribution area for *U. malayanus*, with its distribution located mainly in Yunnan, with recent surveys confirming its presence at higher altitudes (1884 m above sea level) in Tibet (Zhou et al., 2017). Meanwhile, *Ursus thibetanus* prefers broad-leaved or mixed forests, with habitats ranging from low hills to high mountains at altitudes of 2000–3000 m above sea level (Nowak, 1999). Thus, the appearance of these two *Ursus* species implies a mixed forested habitat.

According to stable carbon isotope results from the late Middle Pleistocene site of Tham Wiman Nakin, ungulates such as *Bos gaurus, Capricornis sumatrensis* and *Cervus (Rusa) unicolor*, which are the mixed feeders, can survive in more open C_4 habitats (Pushkina et al., 2010). Thus, their increased proportion in Upper Pubu probably indicates the increased presence of more open grassland. This is perhaps not all that surprising given that Upper Pubu dates primarily to marine isotope stage 6, a major glacial period.

At least two species of rhinocerotids (*Rhinoceros sondaicus*, *Dicerorhinus sumatrensis*) coexisted in Upper Pubu. This coexistence has previously been observed only in Ganxian among the many cave sites in southern China. *R. sondaicus* is an exclusive browser that primarily feeds on shoots, twigs, young foliage, and fruits, preferring high grasses and lowland reedbeds in tropical rainforests where there are ample water sources and mud wallows (Nowak, 1999). *D. sumatrensis* is also a browser, consuming leaves, twigs, and fruits in a diverse range of habitats including lowland rainforests, swamps, and montane moss forests, but consistently stays close to fresh water and salt licks (Nowak, 1999). They both imply a habitat close to water sources.

In brief, the composition of the Upper Pubu mammalian fauna suggests a predominantly forested mosaic-like habitat with some open areas, situated in an overall climate of warmth and humidity. This ecological environment has similarities with the observations made in the Ganxian fauna (Liang et al., 2022), which is slightly older than Upper Pubu. However, the sharp decline in the number of primates and the increase in the proportion of herbivores in Upper Pubu indicate a decrease in forest density and an increase in grassland area at that time. Given that the latest dating results suggest that Upper Pubu mainly falls in MIS 6, a drier environment and more open grassland would be expected, which is consistent with paleoenvironmental implications indicated by the fauna. Further studies will test this hypothesis.

6. Conclusion

The deposits of relatively rapid accumulation in Upper Pubu yielded an abundance of mammal fossils. Interestingly, the age of the fauna is constrained to 210–100 ka (Zhang et al., 2024), which mainly falls in MIS 6. Based on the taxonomic study presented here, the Upper Pubu fossil assemblage sheds light on the characteristics of the mammalian fauna during the terminal Middle Pleistocene in southern China for the first time. Basically, the Artiodactyla-dominated fauna (91.4% of the fauna composition) still retains the typical taxonomic composition of the *Stegodon-Ailuropoda* fauna of southern China. However, faunal comparisons with other late Middle Pleistocene and Late Pleistocene sites in nearby areas exhibit an apparent decline in primates in Upper Pubu, which probably indicates a reduction in forest area and environmental degradation during this period. The palaeoenvironmental reconstruction derived from the composition of the Upper Pubu fauna suggests a primarily forested mosaic habitat under generally warm and humid conditions, but with some open grassland areas. Finally, the observation

of changes in the proportion of extinct elements (including globally and locally) from the Middle Pleistocene to Holocene faunas in the Bubing Basin not only provide insight into the variation in the *Stegodon-Ailuropoda* Faunal Complex in southern China, but also suggests the next logical step will be to divide the late Middle to Late Pleistocene "*Stegodon-Ailuropoda*" mammalian faunas into more formal subunits based on taxonomic variation and biochronology.

Author contributions

Yijing Zhang: identifying and measuring fossil materials, responsible for statistical analysis and figures and tables production, the main author to write this paper. Yaobin Fan: helping paper revision. Yanyan Yao: measuring and drawing the plan of the cave. Chun Tian: taking part in the cave excavation. Hua Liang: measuring and drawing the plan of the cave. Jinyan Li: taking part in the cave excavation. Wei Liao: taking part in the cave excavation and executing pre-experimental treatment. Christopher J. Bae: guiding paper revision. Wei Wang: in charge of cave excavation, the part of stratigraphic description and guiding paper writing.

Funding

This work has been supported by the Major Programme of the National Social Science Foundation of China (20&ZD246), the National Natural Science Foundation of China (42002025), and the Taishan Scholars Project Special Funding.

Declaration of competing interest

The authors declare that they have no known competing financial interests or personal relationships that could have appeared to influence the work reported in this paper.

Acknowledgements

We thank F. Tian (Tiandong County Museum), J.Y. Mo and C. L. Huang (Natural History Museum of Guangxi) for their participation in field investigation and excavation. We would like to thank Y.Q. Liufu, S. W. Xie, M. Shao and Q. Zhou (Natural History Museum of Guangxi) for their assistance in fossil specimen arrangement. We appreciate the comments from two anonymous reviewers which helped to strengthen this manuscript. We alone are responsible for any errors.

Appendix A. Supplementary data

Supplementary data to this article can be found online at https://doi.org/10.1016/j.quascirev.2024.109082.

Data availability

Data will be made available on request.

References

Bacon, A.-M., Antoine, P.-O., Huong, N.T.M., Westaway, K., Tuan, N.A., Duringer, P., Zhao, J., Ponche, J.-L., Dung, S.C., Nghia, T.H., Minh, T.T., Son, P.T., Boyon, M., Thuy, N.T.K., Blin, A., Demeter, F., 2018a. A rhinocerotid-dominated megafauna at the MIS6-5 transition: the late Middle Pleistocene Coc Muoi assemblage, Lang Son province, Vietnam. Quat. Sci. Rev. 186, 123–141. https://doi.org/10.1016/j.quascirev.2018.02.017.

Bacon, A.-M., Bourgon, N., Dufour, E., Zanolli, C., Duringer, P., Ponche, J.-L., Antoine, P.-O., Shackelford, L., Huong, N.T.M., Sayavonkhamdy, T., Patole-Edoumba, E., Demeter, F., 2018b. Nam Lot (MIS 5) and Duoi U'Oi (MIS 4) Southeast Asian sites revisited: Zooarchaeological and isotopic evidences. Palaeogeogr. Palaeoclimatol. Palaeoecol., Cenozoic Climate Change in Eastern Asia - PART II 512, 132–144. https://doi.org/10.1016/j.palaeo.2018.03.034.

Bacon, A.-M., Demeter, F., Duringer, P., Helm, C., Bano, M., Vu The, L., Kim Thuy, N.T., Antoine, P.O., Thi Mai, B., Huong, N.T.M., Dodo, Y., Chabaux, F., Rihs, S., 2008. The Late Pleistocene Duoi U'Oi cave in northern Vietnam: palaeontology, sedimentology, taphonomy and palaeoenvironments. Quat. Sci. Rev. 27, 1627–1654. https://doi.org/10.1016/j.quascirev.2008.04.017.

Bacon, A.-M., Duringer, P., Antoine, P.-O., Demeter, F., Shackelford, L., Sayavongkhamdy, T., Sichanthongtip, P., Khamdalavong, P., Nokhamaomphu, S., Sysuphanh, V., Patole-Edoumba, E., Chabaux, F., Pelt, E., 2011. The Middle Pleistocene mammalian fauna from Tam Hang karstic deposit, northern Laos: new data and evolutionary hypothesis. Quat. Int. 245, 315–332. https://doi.org/10.1016/j.quaint.2010.11.024.

Badoux, D.M., 1959. Fossil Mammals from Two Deposits at Punung (Java) with Some Remarks on Migrations and Evolution of Mammals during the Quaternary in South East Asia (Dissertation). Utrecht University, Utrecht.

Bae, C.J., 2024. The Paleoanthropology of Eastern Asia. University of Hawaii Press, Honolulu.

Bae, C.J., Wang, W., Zhao, J., Huang, S., Tian, F., Shen, G., 2014. Modern human teeth from Late Pleistocene Luna Cave (Guangxi, China). Quat. Int. 354, 169–183. https://doi.org/10.1016/j.quaint.2014.06.051.

Cai, Y., Qiang, X., Wang, X., Jin, C., Wang, Y., Zhang, Y., Trinkaus, E., An, Z., 2017. The age of human remains and associated fauna from Zhiren Cave in Guangxi, southern China. Quat. Int. 434, 84–91. https://doi.org/10.1016/j.quaint.2015.12.088.

Chen, G., Wang, W., Mo, J., Huang, Z., Tian, F., Huang, W., 2002. Pleistocene vertebrate fauna from Wuyun Cave of Tiandong county. Guangxi. Vertebr. Palasiat. 40, 42–51. https://doi.org/10.19615/j.cnki.1000-3118.2002.01.007.

Cheng, H., Edwards, R.L., Sinha, A., Spötl, C., Yi, L., Chen, S., Kelly, M., Kathayat, G., Wang, X., Li, X., Kong, X., Wang, Y., Ning, Y., Zhang, H., 2016. The Asian monsoon over the past 640,000 years and ice age terminations. Nature 534, 640–646. https://doi.org/10.1038/nature18591.

Colbert, E.H., 1943. Pleistocene vertebrates collected in Burma by the American Southeast Asiatic expedition. Trans. Am. Phil. Soc. 32, 395–429.

Colbert, E.H., 1942. Sections of geology and mineralogy: the Pleistocene faunas of Asia and their relationships to early man. Trans. N. Y. Acad. Sci. 5, 1–10. https://doi.org/10.1111/j.2164-0947.1942.tb00857.x.

Colbert, E.H., Hooijer, D.A., 1953. Pleistocene mammals from the limestone fissures of Szechwan, China. Bull. Am. Mus. Nat. Hist. 102, 1–134.

Deng, C., Hao, Q., Guo, Z., Zhu, R., 2019. Quaternary integrative stratigraphy and timescale of China. Sci. China Earth Sci. 62, 324–348. https://doi.org/10.1007/s11430-017-9195-4.

Dong, W., Wang, Y., Bai, W., Zhang, Y., Liu, J., Jin, C., 2020. Late early Pleistocene artiodactyls associated with *Gigantopithecus* from Queque cave, Chongzuo, Guangxi, south China. Acta Anthropol. Sin. 39, 306–318.

Fan, Y., Li, J., Gong, R., Shen, G., Liao, W., Wang, W., 2022a. Taphonomy and biochronology of the Late Pleistocene mammalian fauna at Baolai cave. In: Basin, Bubing (Ed.), Hist. Biol.. https://doi.org/10.1080/08912963.2022.2145561.

Fan, Y., Shao, Q., Bacon, A.-M., Liao, W., Wang, W., 2022b. Late Pleistocene large-bodied mammalian fauna from Mocun cave in south China: Palaeontological, chronological and biogeographical implications. Quat. Sci. Rev. 294, 107741. https://doi.org/10.1016/j.quascirev.2022.107741.

Ge, J., Deng, C., Wang, Y., Shao, Q., Zhou, X., Xing, S., Pang, H., Jin, C., 2020. Climate-influenced cave deposition and human occupation during the Pleistocene in Zhiren Cave, southwest China. Quat. Int. 559, 14–23. https://doi.org/10.1016/j.quaint.2020.01.018.

Gu, Y., 1986. Preliminary research on the fossil Gibbon of Pleistocene China. Acta Anthropol. Sin. 5, 208–219.

Gu, Y., Huang, W., Chen, D., Guo, X., Jablonski, N.G., 1996. Pleistocene fossil primates from Luoding, Guangdong. Vertebr. Palasiat. 34, 235–250.

Han, D., 1987. Artiodactyla fossils from Liucheng *Gigantopithecus* cave in Guangxi. Mem. Inst. Vertebr. Paleontol. Paleoanthropol. Acad. Sinica 18, 135–208. Science Press, Bejing.

Han, D., 1982. Mammalian fossils from Tahsin County, Guangxi. Vertebr. Palasiat. 20, 58–64+96.

Han, D., Xu, C., Yi, G., 1975. Quaternary mammal fossils from Bijiashan, Liuzhou, Guangxi. Vertebr. Palasiat. 13, 250-256+283-284.

Han, F., Bahain, J.-J., Deng, C., Boëda, É., Hou, Y., Wei, G., Huang, W., Garcia, T., Shao, Q., He, C., Falguères, C., Voinchet, P., Yin, G., 2017. The earliest evidence of hominid settlement in China: combined electron spin resonance and uranium series (ESR/U-series) dating of mammalian fossil teeth from Longgupo cave. Quat. Int., Quaternary Biostratigraphy in East Asia: A Multidisciplinary Research Approach on Gigantopithecus Fauna and Human Evolution 434, 75–83. https://doi.org/10.1016/j.quaint.2015.02.025.

Harrison, T., Jin, C., Zhang, Y., Wang, Y., Zhu, M., 2014. Fossil *Pongo* from the Early Pleistocene *Gigantopithecus* fauna of Chongzuo, Guangxi, southern China. Quat. Int. 354, 59–67. https://doi.org/10.1016/j.quaint.2014.01.013.

Harrison, T., Zhang, Y., Yang, L., Yuan, Z., 2021. Evolutionary trend in dental size in fossil orangutans from the Pleistocene of Chongzuo, Guangxi, southern China. J. Hum. Evol. 161, 103090. https://doi.org/10.1016/j.jhevol.2021.103090.

Hooijer, D.A., 1948. Prehistoric teeth of man and of the orang-utan from Central Sumatra, with notes on the fossil orang-utan from Java and Southern China. Zool. Meded. 29, 175–301.

Hu, C., Qi, T., 1978. Gongwangling Pleistocene Mammalian Fauna of Lantian. Science Press, Shaanxi. Beijing.

Huang, W., Ciochon, R., Gu, Y., Larick, R., Fang, Q., Schwarcz, H., Yonge, C., de Vos, J., Rink, W., 1995. Early *Homo* and associated artefacts from Asia. Nature 378, 275–278. https://doi.org/10.1038/378275a0.

Huang, W., Fang, Q., 1991. Wushan Hominid Site. China Ocean Press, Beijing.

Ji, H., 1977. The division of Quaternary mammalian faunas in South China. Vertebr. Palasiat. 15, 271–277.

Jiangzuo, Q., Cong, H., Ma, R., Feng, H., Liu, J., 2014. Middle and Late Pleistocene sun bears (Ursidae, Carnivora) from southern China. In: Dong, W. (Ed.), Proceedings of the Fourteenth Annual Meeting of the Chinese Society of Vertebrate Paleontology. Presented at the the Fourteenth Annual Meeting of the Chinese Society of Vertebrate Paleontology. China Ocean Press, Beijing, pp. 119–134. https://doi.org/10.13140/2.1.1868.5126.

Jiangzuo, Q., Liu, J., Chen, J., 2019. Morphological homology, evolution and proposed nomenclature for bear dentition. Acta Palaeontol. Pol. 64, 693–710. https://doi.org/10.4202/app.00629.2019.

Jiangzuo, Q., Liu, J., Wagner, J., Chen, J., 2018a. Taxonomical revision of "Arctonyx" fossil remains from the Liucheng *Gigantopithecus* Cave (South China) by means of morphotype and morphometrics, and a review of Late Pliocene and Early Pleistocene Meles fossil records in China. Palaeoworld 27, 282–300. https://doi.org/10.1016/j.palwor.2017.12.001.

Jiangzuo, Q., Zhang, B., Deng, L., Chen, X., Wen, J., Tong, H., 2018b. Fossil carnivora (mammalia) from Yangjiawan cave 2, Pingxiang, Jiangxi, with remarks about the tooth identification of quaternary carnivores. In: Dong, W. (Ed.), Proceedings of the Sixteenth Annual Meeting of the Chinese Society of Vertebrate Paleontology. Presented at the the Sixteenth Annual Meeting of the Chinese Society of Vertebrate Paleontology. China Ocean Press, Beijing, pp. 119–146.

Jin, C., Pan, W., Zhang, Y., Cai, Y., Xu, Q., Tang, Z., Wang, W., Wang, Y., Liu, J., Qin, D., Lawrence Edwards, R., Cheng, H., 2009a. The *Homo sapiens* Cave hominin site of Mulan Mountain, Jiangzhou District, Chongzuo, Guangxi with emphasis on its age. Chin. Sci. Bull. 54, 3848–3856. https://doi.org/10.1007/s11434-009-0641-1.

Jin, C., Qin, D., Pan, W., Tang, Z., Liu, J., Wang, Y., Deng, C., Zhang, Y., Dong, W., Tong, H., 2009b. A newly discovered *Gigantopithecus* fauna from Sanhe Cave, Chongzuo, Guangxi, South China. Sci. Bull. 54, 1–10. https://doi.org/10.1007/s11434-008-0531-y.

Jin, C., Wang, Y., Deng, C., Harrison, T., Qin, D., Pan, W., Zhang, Y., Zhu, M., Yan, Y., 2014. Chronological sequence of the early Pleistocene *Gigantopithecus* faunas from cave sites in the Chongzuo, Zuojiang River area, South China. Quat. Int. 354, 4–14. https://doi.org/10.1016/j.quaint.2013.12.051.

Jin, C., Zheng, J., Wang, Y., Xu, Q., 2008. The stratigraphic distribution and zoogeography of the Early Pleistocene mammalian fauna from South China. Acta Anthr. Sin 27, 304–317.

Kahlke, H.D., 1961. On the Complex of the *Stegodon-Ailuropoda*-Fauna of Southern China and the Chronological Position of *Gigantopithecus blacki* von Koenigswald. Vertebr. Palasiat. 83–108.

Kong, L., Shen, G., Wang, W., Li, D., Zhao, J., 2012. U-series dating of the Shizi Cave and Age of the Third Terrace of the Bubing and Baise Basins, Guangxi, China. Earth Environ. 40, 349–353, 10.14050/j.cnki.1672-9250.2012.03.022.

Li, Y., Pei, S., Tong, H., Yang, X., Cai, Y., Liu, W., Wu, X., 2013. A preliminary report on the 2011 excavation at Houbeishan Fuyan Cave, Daoxian, Hunan Province. Acta Anthropol. Sin. 32, 133–143.

Liang, H., Harrison, T., Shao, Q., Bahain, J.-J., Zhao, J., Bae, C.J., Liao, W., Wang, W., 2023. Middle Pleistocene *Pongo* from Ganxian Cave in southern China with implications for understanding dental size evolution in orangutans. J. Hum. Evol. 178, 103348. https://doi.org/10.1016/j.jhevol.2023.103348.

Liang, H., Liao, W., Shao, Q., Chen, Q., Tian, C., Yao, Y., Li, J., Wang, W., 2022. New discovery of a late Middle Pleistocene mammalian fauna in Ganxian Cave, Southern China. Hist. Biol. 1–18. https://doi.org/10.1080/08912963.2022.2139180.

Liang, H., Liao, W., Yao, Y., Bae, C.J., Wang, W., 2020. A late Middle Pleistocene mammalian fauna recovered in northeast Guangxi, southern China: implications for regional biogeography. Quat. Int. 563, 29–37.

Liao, W., Feng, Y., Zhao, J., Jiang, T., Yao, Y., Liang, H., Nguyen, A.D., Bae, C.J., Wang, W., 2020. Combined U-series dating of cave pearls and mammal fossils: constraint on the age of a late middle pleistocene *Ailuropoda–Stegodon* fauna from the Diaozhongyan Cave, Guangxi, South China. Quat. Geochronol. 60, 101111.

Liao, W., Harrison, T., Yao, Y., Liang, H., Tian, C., Feng, Y., Li, S., Bae, C.J., Wang, W., 2022. Evidence for the latest fossil *Pongo* in southern China. J. Hum. Evol. 170, 103233. https://doi.org/10.1016/j.jhevol.2022.103233.

Liu, W., Jin, C.Z., Zhang, Y.Q., Cai, Y.J., Xing, S., Wu, X.J., Cheng, H., Edwards, R.L., Pan, W.S., Qin, D.G., An, Z.S., Trinkaus, E., Wu, X.Z., 2010. Human remains from Zhirendong, South China, and modern human emergence in East Asia. Proc Natl Acad Sci U S A 107, 19201–19206. https://doi.org/10.1073/pnas.1014386107.

Maglio, V.J., 1973. Origin and evolution of the Elephantidae. Trans. Am. Phil. Soc. 63, 1–149. https://doi.org/10.2307/1006229.

Matthew, W.D., Granger, W., 1923. New fossil mammals from the Pliocene of Sze-Chuan, China. Bull. Am. Mus. Nat. Hist. 48, 563–598.

Nakazawa, Y., Bae, C.J., 2018. Quaternary paleoenvironmental variation and its impact on initial human dispersals into the Japanese Archipelago. Palaeogeogr. Palaeoclimatol. Palaeoecol., Cenozoic Climate Change in Eastern Asia - PART II 512, 145–155. https://doi.org/10.1016/j.palaeo.2017.12.030.

Norton, C.J., 2000. The current state of Korean paleoanthropology. J. Hum. Evol. 38, 803–825. https://doi.org/10.1006/jhev.1999.0390.

Norton, C.J., Jin, C., Wang, Y., Zhang, Y., 2010. Rethinking the Palearctic-oriental biogeographic boundary in quaternary China. In: Norton, C.J., Braun, D.R. (Eds.), Asian Paleoanthropology: from Africa to China and beyond, Vertebrate Paleobiology and Paleoanthropology Series. Springer Press, Dordrecht, The Netherlands, pp. 81–100. https://doi.org/10.1007/978-90-481-9094-2_7.

Nowak, R.M., 1999. Walker's Mammals of the World. The John Hopkins University Press, London.

Pan, Y., 2021. An α-taxonomy study of the late Middle Pleistocene mammalian fauna from the Yixiantian Cave. Chongzuo, Guangxi Zhuang Autonomous Region (Master's Thesis). University of Chinese Academy of Sciences, Beijing.

Pan, Y., Zhang, Y., Yang, L., Takai, M., Harrison, T., Westaway, K., Jin, C., 2023. Preliminary description of a late Middle Pleistocene mammalian fauna prior to the extinction of *Gigantopithecus blacki* from the Yixiantian Cave, Guangxi ZAR, South China. Anat. Rec. 1–26. https://doi.org/10.1002/ar.25200.

Pei, W., Woo, J., 1956. New materials of *Gigantopithecus* teeth from South China. Acta Palaeontol. Sin. 4, 477-490+655-661.

Pei, W.C., 1935. Fossil mammals from the Kwangsi caves. Bull. Geol. Soc. China 14, 413–425.

Pushkina, D., Bocherens, H., Chaimanee, Y., Jaeger, J.-J., 2010. Stable carbon isotope reconstructions of diet and paleoenvironment from the late Middle Pleistocene Snake Cave in Northeastern Thailand. Naturwissenschaften 97, 299–309. https://doi.org/10.1007/s00114-009-0642-6.

Qiu, Z., 2006. Quaternary environmental changes and evolution of large mammals in North China. Vertebr. Palasiat. 44, 109–132.

Rink, W.J., Wang, W., Bekken, D., Jones, H.L., 2008. Geochronology of *Ailuropoda–Stegodon* fauna and *Gigantopithecus* in Guangxi Province, southern China. Quat. Res. 69, 377–387. https://doi.org/10.1016/j.yqres.2008.02.008.

Roth, V.L., Shoshani, J., 1988. Dental identification and age determination in *Elephas maximus*. J. Zool. 214, 567–588. https://doi.org/10.1111/j.1469-7998.1988.tb03760.x.

Shao, Q., Bahain, J.-J., Wang, W., Zhu, M., Voinchet, P., Lin, M., Douville, E., 2015. Coupled ESR and U-series dating of early Pleistocene *Gigantopithecus* faunas at Mohui and Sanhe Caves, Guangxi, southern China. Quat. Geochronol. 30, 524–528. https://doi.org/10.1016/j.quageo.2015.04.008.

Shao, Q., Wang, W., Deng, C., Voinchet, P., Lin, M., Zazzo, A., Douville, E., Dolo, J.-M., Falguères, C., Bahain, J.-J., 2014. ESR, U-series and paleomagnetic dating of *Gigantopithecus* fauna from Chuifeng Cave, Guangxi, southern China. Quat. Res. 82, 270–280. https://doi.org/10.1016/j.yqres.2014.04.009.

Shao, Q., Wang, Y., Voinchet, P., Zhu, M., Lin, M., Rink, W.J., Jin, C., Bahain, J.-J., 2017. U-series and ESR/U-series dating of the *Stegodon–Ailuropoda* fauna at Black Cave, Guangxi, southern China with implications for the timing of the extinction of *Gigantopithecus blacki*. Quat. Int. 434, 65–74.

Smith, H.E., Price, G.J., Duval, M., Westaway, K., Zaim, J., Rizal, Y., Aswan, Puspaningrum, M.R., Trihascaryo, A., Stewart, M., Louys, J., 2021. Taxonomy, taphonomy and chronology of the Pleistocene faunal assemblage at Ngalau Gupin cave, Sumatra. Quat. Int. 603, 40–63. https://doi.org/10.1016/j.quaint.2021.05.005.

Storm, P., de Vos, J., 2006. Rediscovery of the Late Pleistocene Punung hominin sites and the discovery of a new site Gunung Dawung in East Java. Senckenberg. Lethaea 86, 271–281.

Sun, J., Zhang, B., Chen, X., Deng, L., Wen, J., Tong, H., 2021a. New fossils of Late Pleistocene *Sus scrofa* from Yangjiawan Cave 2, Jiangxi, China. Vertebr. Palasiat. 59, 64–80.

Sun, L., Deng, C., Wang, W., Liu, C., Kong, Y., Wu, B., Liu, S., Ge, J., Qin, H., Zhu, R., 2017. Magnetostratigraphy of Plio–pleistocene fossiliferous cave sediments in the Bubing Basin, southern China. Quat. Geochronol. 37, 68–81. https://doi.org/10.1016/j.quageo.2016.09.007.

Sun, L., Wang, Y., Liu, C., Zuo, T., Ge, J., Zhu, M., Jin, C., Deng, C., Zhu, R., 2014. Magnetochronological sequence of the Early Pleistocene *Gigantopithecus* faunas in Chongzuo, Guangxi, southern China. Quat. Int. 354, 15–23. https://doi.org/10.1016/j.quaint.2013.08.049.

Sun, X., Wen, S., Lu, C., Zhou, B., Curnoe, D., Lu, H., Li, Hong-chun, Wang, W., Cheng, H., Yi, S., Jia, X., Du, P., Xu, X., Lu, Yi-ming, Lu, Ying, Zheng, H., Zhang, H., Sun, C., Wei, L., Han, F., Huang, J., Edwards, R.L., Jin, L., Li, Hui, 2021b. Ancient DNA and multimethod dating confirm the late arrival of anatomically modern humans in southern China. Proc. Natl. Acad. Sci. 118, e2019158118. https://doi.org/10.1073/pnas.2019158118.

Suraprasit, Kantapon, Jaeger, J.-J., Chaimanee, Y., Chavasseau, O., Yamee, C., Tian, P., Panha, S., 2016. The Middle Pleistocene vertebrate fauna from Khok Sung (Nakhon Ratchasima, Thailand): biochronological and paleobiogeographical implications. ZooKeys 613, 1–157. https://doi.org/10.3897/zookeys.613.8309.

Suraprasit, K., Jaeger, J.-J., Chaimanee, Y., Sutcharit, C., 2021. Taxonomic reassessment of large mammals from the Pleistocene *Homo*-bearing site of Tham Wiman Nakin (Northeast Thailand): relevance for faunal patterns in mainland Southeast Asia. Quat. Int. 603, 90–112. https://doi.org/10.1016/j.quaint.2020.06.050.

Swindler, D.R., 2002. Primate Dentition: an Introduction to the Teeth of Non-human Primates. Cambridge University Press, Cambridge.

Takai, M., Zhang, Y., Kono, R.T., Jin, C., 2014. Changes in the composition of the Pleistocene primate fauna in southern China. Quat. Int. 354, 75–85. https://doi.org/10.1016/j.quaint.2014.02.021.

Tong, H., 2005. Dental characters of the Quaternary tapirs in China, their significance in classification and phylogenetic assessment. Geobios 38, 139–150. https://doi.org/10.1016/j.geobios.2003.07.006.

Tong, H., 2004. Tapiridae. In: Zheng, S. (Ed.), Jianhsi Hominid Site. Science Press, Beijing, pp. 233–250.

Tong, H., Guérin, C., 2009. Early Pleistocene *Dicerorhinus sumatrensis* remains from the Liucheng *Gigantopithecus* Cave, Guangxi, China. Geobios 42, 525–539. https://doi.org/10.1016/j.geobios.2009.02.001.

Tong, H., Wu, X., Dong, Z., Sheng, J., Jin, Z., Pei, S., Liu, W., 2018. Preliminary report on the mammalian fossils unearthed from the ancient human site of Hualong Cave in DongZhi, Anhui. Acta Anthropol. Sin. 37, 284–305.

Tougard, C., Montuire, S., 2006. Pleistocene paleoenvironmental reconstructions and mammalian evolution in South-East Asia: focus on fossil faunas from Thailand. Quat. Sci. Rev. 25, 126–141. https://doi.org/10.1016/j.quascirev.2005.04.010.

Van den Bergh, G.D., 1999. The Late Neogene elephantoid-bearing faunas of Indonesia and their palaeozoogeographic implicationsimplications: a study of the terrestrial

faunal succession of Sulawesi, Flores and Java, including evidence for early hominid dispersal east of Wallace's Line. Scr. Geol. 117, 1–388.
van der Made, J., 1996. Listriodontinae (Suidae, Mammalia), their evolution, systematics and distribution in time and space. Contrib. Tert. Quat. Geol. 33, 3–254.
Wang, C., Zhao, L., Jin, C., Wang, Y., Qin, D., Pan, W., 2014. New discovery of Early Pleistocene orangutan fossils from Sanhe Cave in Chongzuo, Guangxi, southern China. Quat. Int., Multidisciplinary Perspectives on the Gigantopithecus Fauna and Quaternary Biostratigraphy in East Asia 354, 68–74. https://doi.org/10.1016/j.quaint.2014.06.020.
Wang, W. (Ed.), 2013. The Early Pleistocene Mohui Cave Site in Tiandong County, Guangxi, South China. Science Press, Beijing.
Wang, W., Potts, R., Yuan, B., Huang, W., Cheng, H., Edwards, R.L., Ditchfield, P., 2007. Sequence of mammalian fossils, including hominoid teeth, from the Bubing Basin caves, South China. J. Hum. Evol. 52, 370–379. https://doi.org/10.1016/j.jhevol.2006.10.003.
Wang, Y., Jin, C., Pan, W., Qin, D., Yan, Y., Zhang, Y., Liu, J., Dong, W., Deng, C., 2017a. The Early Pleistocene *Gigantopithecus-Sinomastodon* fauna from Juyuan karst cave in Boyue Mountain, Guangxi, South China. Quat. Int. 434, 4–16. https://doi.org/10.1016/j.quaint.2015.11.071.
Wang, Y., Zhao, L., Du, B., Zhang, L., Wang, X., Cai, H., 2017b. New proboscidean remains associated with *Homo sapiens* from the Mawokou Cave in Bijie, Guizhou Province of south-western China. Acta Anthropol. Sin. 36, 414–425. https://doi.org/10.16359/j.cnki.cn11-1963/q.2017.0045.
Yan, Y., Wang, Y., Jin, C., Mead, J.I., 2014. New remains of *Rhinoceros* (Rhinocerotidae, Perissodactyla, Mammalia) associated with *Gigantopithecus blacki* from the Early Pleistocene Yanliang Cave, Fusui, South China. Quat. Int. 354, 110–121. https://doi.org/10.1016/j.quaint.2014.01.004.
Yan, Y., Zhang, Yang, Jin, C., Zhang, Yingqi, Wang, Y., 2020. The first fossil record of *Rhinoceros sondaicus* from the Pleistocene of China. Geol. Rev. 66, 198–206.
Yao, Y., Fan, Y., Bae, C.J., Tian, C., Liang, H., Chen, J., Zhang, B., Wei, S., Shao, Q., Liao, W., Wang, W., 2023. Early Mid-Pleistocene mammal fauna from Yanlidong Cave, South China. Hist. Biol 1–18. https://doi.org/10.1080/08912963.2023.2185886.
Yao, Y., Liao, W., Bae, C.J., Sun, X., Feng, Y., Tian, C., Li, J., Wei, S., Wang, W., 2020. New discovery of Late Pleistocene modern human teeth from Chongzuo, Guangxi, southern China. Quat. Int., Dispersal Barriers into Southeast Asia during the Late Pleistocene 563, 5–12. https://doi.org/10.1016/j.quaint.2020.02.002.
Zhang, B., Chen, X., Tong, H.-W., 2018a. Tooth remains of Late Pleistocene moschid and cervid (Artiodactyla, Mammalia) from Yangjiawan and Fuyan Caves of southern China. Quat. Int. 490, 21–32.
Zhang, Y., Jin, C., Cai, Y., Kono, R., Wang, W., Wang, Y., Zhu, M., Yan, Y., 2014. New 400–320 ka *Gigantopithecus blacki* remains from Hejiang Cave, Chongzuo City, Guangxi, South China. Quat. Int. 354, 35–45. https://doi.org/10.1016/j.quaint.2013.12.008.
Zhang, Y., Jin, C., Wang, Y., Ortiz, A., He, K., Harrison, T., 2018b. Fossil gibbons (Mammalia, Hylobatidae) from the Pleistocene of Chongzuo, Guangxi, China. Vertebr. Palasiat. 56, 248–263. https://doi.org/10.19615/j.cnki.1000-3118.180403.
Zhang, Y., Westaway, K.E., Haberle, S., Lubeek, J.K., Bailey, M., Ciochon, R., Morley, M. W., Roberts, P., Zhao, J., Duval, M., Dosseto, A., Pan, Y., Rule, S., Liao, W., Gully, G. A., Lucas, M., Mo, J., Yang, L., Cai, Y., Wang, W., Joannes-Boyau, R., 2024. The demise of the giant ape *Gigantopithecus blacki*. Nature 1–5. https://doi.org/10.1038/s41586-023-06900-0.
Zhao, Z., Liu, X., Wang, L., 1981. Human Fossils and associated fauna of Jiulengshan Hill. Guangxi. Vertebr. Palasiat. 19, 45-54+105-106.
Zheng, S., 2004. Jianshi Hominid Site. Science Press, Beijing.
Zhou, M., 1957. The nature and contrast of Tertiary and Early Quaternary mammalian fauna in South China. Chin. Sci. Bull. 13, 394–400.
Zhou, Z., Huang, Z., Hu, Y., Li, J., Wu, J., Hu, H., 2017. New record of sun bear (*Helarctos malayanus*) in Jilong County, Tibet, China. Acta Theriol. Sin. 37, 414–416.
Zhu, M., Yan, Y., Liu, Y., Tang, Z., Qin, D., Jin, C., 2017. The new carnivore remains from the Early Pleistocene Yanliang *Gigantopithecus* fauna, Guangxi, South China. Quat. Int. 434, 17–24. https://doi.org/10.1016/j.quaint.2015.01.009.